Accepted manuscrip. Published manuscrip link:
http://www.sciencedirect.com/science/article/pii/S0925400515306948
doi:10.1016/j.snb.2015.11.116

Colorimetric detection and determination of Fe(III), Co(II), Cu(II) and Sn(II) in aqueous media by acrylic polymers with pendant terpyridine motifs

Miriam Trigo-López, Asunción Muñoz, Saturnino Ibeas, Felipe Serna, Félix Clemente García and José Miguel García*

Departamento de Química, Facultad de Ciencias, Universidad de Burgos, Plaza de Misael Bañuelos s/n, 09001 Burgos, Spain. Fax: (+) 34 947 258 831, Tel: (+) 34 947 258 085. E-mail: jmiguel@ubu.es

Graphical abstract

ABSTRACT

Colorimetric cation responsive water soluble polymers and manageable films or membranes have been designed. The sensory materials respond with a colour change to the presence in water of Fe(III), Co(II), Cu(II), and Sn(II). The colour change is specific of each metal cation, and enables its identification (purple for iron, orange for cobalt, green for copper, and yellow for tin). The design of the materials relies on an addition monomer having a terpyridine moiety, which behaves as a dye in presence of transition metal cations due to its proven chelating capability toward these species and the colour development that always accompany the metallic complex formation. Water solutions of the sensory linear polymers allow for the UV/vis titration of Fe(III), Co(II), Cu(II),

Accepted manuscrip. Published manuscrip link:
http://www.sciencedirect.com/science/article/pii/S0925400515306948
doi:10.1016/j.snb.2015.11.116

and Sn(II) with a limit of detection of $1.3x10^{-7}$, $6.4x10^{-8}$, $1.3x10^{-5}$ and $1.4x10^{-5}$ M, respectively. On the other hand, sensory kits, cut from sensory membranes, permitted the visual quantification of the cations in a dynamic range of five decades ($1x10^{-7}$ - $5x10^{-3}$ M) for Fe(III) and Co(II) and of two decades ($9x10^{-5}$ - $9x10^{-3}$ M) for Cu(II) and Sn(II). Titration curves can also be drawn from a picture taken to the sensory kits with a smartphone, by using the digital colour definition of the materials as analytical signal. Also, after entering into contact with hands, shapes of metallic objects (iron and cobalt containing tools) can be colour revealed by pressing the hands on paper or cotton fabrics wetted with water solutions of the linear sensory polymer.

Keywords

Sensory polymers, terpyridine, cation detection, forensic applications

1. INTRODUCTION

The costless, *in-situ*, and fast detection and quantification of transition metal cations in pure water are of the utmost environmental, industrial, and health importance. Traditional techniques, such as atomic absorption spectroscopy (AAS) or inductively coupled plasma mass spectrometry (ICP-MS), enable the selective and precise detection and quantification of the mentioned chemical species. However, they are heavy, bulky, extremely expensive techniques and require trained personnel. On the other hand, chemical sensors have become a simple species detection method for non-trained personnel, especially if the transduction is chromogenic (i.e., by a colour change) and the detection can be carried out visually.

Chemical sensors are an emerging technology with expanding applicability to a number of fields, such as civil security, environmental control and remediation, medicine, and industrial control. Moreover, sensory polymers, which are

Accepted manuscrip. Published manuscrip link:
http://www.sciencedirect.com/science/article/pii/S0925400515306948
doi:10.1016/j.snb.2015.11.116

macromolecules that have receptor motifs (or binding sites) in their structure, represent a step further and show significant advances over discrete (or low molecular mass) chemosensors. Thus, polymers can be prepared or transformed into films, coatings or finished sensory materials with different shapes. Distinct polymer geometries are achievable (linear, spherical, and tridimensional crosslinked network). They can be easily designed to work in hydrophobic or hydrophilic environments and can be used to sense both vapours and liquids. Also, they exhibit collective properties sensitive to minor perturbations. Finally, their sensory moieties cannot migrate with the concomitant increase in the performance stability along time, improve in the thermal and chemical resistance, and can be easily reused.

Chemosensory polymers following a research methodology based on a guaranteed of success strategy have been prepared. That is to say, once chemical species to be detected are selected, the so-called targets, fully confident receptors for such targets are looked in scientific literature to find, usually, discrete organic molecules that are insoluble in water; then, their chemical structure is slightly modified by including a polymerizable group; and finally it is copolymerized with commercial hydrophilic and hydrophobic monomers to have water soluble linear polymers and crosslinked membranes with gel structures that allow for the detection in 100% water. The target species for this work are transition metal cations (Fe(III), Co(II), Cu(II) and Sn(II)), and the receptor core is based on a terpyridine (2,2':6',2''-terpyridine, tpy) motif.

Morgan and Burstal isolated tpy and described its purple complex with iron(II) in the 1930s [1]. Since then tpy has become one of the most used ligands with multiple applications in different research and technological areas, such as coordination polymers [2-4]; sensors for anion [5-8], cations [9-17], both[18,19], and biomolecules

Accepted manuscrip. Published manuscrip link:
http://www.sciencedirect.com/science/article/pii/S0925400515306948
doi:10.1016/j.snb.2015.11.116

[20,21]; gelation and solvochromic sensors [22]; luminescent converters [23-25]; photon harvesting [26] and catalysis [27]. Terpyridine derivatives are multivalent pyridine ligands that exhibit strong binding affinity toward a broad set of transition metal cations. This extremely strong interactions come both from the dπ-dπ* back bonding of the cations to the *N*-heterocycle rings and from the chelate effect [28,29].

Here, the tpy structure has been modified with a polymerizable methacrylamide group and two kind of chromogenic sensory materials have been prepared: linear polymers and solid film-shaped dense membranes comprised of crosslinked polymer networks. The tpy-monomer (~1% mol) was copolymerized with a balance of hydrophilic and hydrophobic commercial co-monomers (~99% mol) to give linear copolymers and networks (membranes). The linear polymers are water soluble. The membranes are solid, exhibit gel behaviour, and can be used to prepare manageable solid sensory kits. Both type of materials respond with development of different colour depending on the presence of Fe(III), Co(II), Cu(II) and Sn(II) in 100% water under controlled acidic conditions. The detection in 100% water is relevant for real-life environmental applications, whereas the acidic conditions avoid the analytical complexity of dealing with presence of different species of each cation (for instance, for iron at pH 2 only Fe^{3+} species are present, while at pH > 2 there are different equilibria of Fe^{3+}, $Fe(OH)^{2+}$, $Fe(OH)_2^{+}$, and $Fe(OH)_3$). Also, the usual presence in most research studies of organic solvents, due to the insolubility in water of conventional probes, influence the selectivity of the tpy core [30].

2. EXPERIMENTAL PART

2.1. Materials

Accepted manuscrip. Published manuscrip link:
http://www.sciencedirect.com/science/article/pii/S0925400515306948
doi:10.1016/j.snb.2015.11.116

All materials and solvents were commercially available and used as received, unless otherwise indicated: 2-acetylpyridine (98%, Alfa Aesar), iodine (≥ 99.8%, Sigma-Aldrich), 4-nitrobenzaldehyde (99% Alfa Aesar), ammonium acetate (97%, Alfa Aesar), tin chloride anhydrous (98% , Alfa Aesar), methacryloyl chloride (97%, Alfa Aesar), triethylamine (TEA) (≥ 99%, Aldrich), pyridine (≥ 99%, Probus), sodium hydroxide (99.9%, VWR-Prolabo), hydrochloric acid (37%, VWR-Prolabo), *N*-methyl-2-pyrrolidone (NMP) (99%, Aldrich), ethanol (99.97%, VWR-Prolabo), diethyl ether (≥ 99,5%, Aldrich), $SnCl_2$ anhydrous (98%, Alfa Aesar), $Fe(NO_3)_3 \cdot 9H_2O$ (VWR-Prolabo), $Cu(NO_3)_2 \cdot 3H_2O$ (98%, Sigma-Aldrich), $Co(NO_3)_2 \cdot 6H_2O$ (≥ 99%, Labkem), NaCl (≥ 99%, Sigma-Aldrich), KCl (99.5%, Scharlau), $Al(NO_3)_2 \cdot 9H_2O$ (≥ 989%, Sigma-Aldrich), $Pb(NO_3)_2$ (≥ 99%, Fluka), LiCl (≥ 99%, Sigma-Aldrich), $Zn(NO_3)_2 \cdot 6H_2O$ (98%, Aldrich), $Mg(NO_3)_2 \cdot 6H_2O$ (≥ 99%, Labkem), $Cd(NO_3)_2$ (98.5%, Alfa Aesar), $Ni(NO_3)_2 \cdot 6H_2O$ (98.5%, Sigma-Aldrich), methyl methacrylate (**MMA**) (99%, Aldrich), 1-vinyl-2-pyrrolidone (**VP**) (≥ 99%, Sigma-Aldrich), ethylene glycol dimethacrylate (**EGDMMA**) (98%, Sigma-Aldrich), Azo-bis-isobutyronitrile (AIBN, ≥ 98%, Aldrich) was recrystallised twice from methanol.

2.2. Instrumentation and measurements

^{1}H and ^{13}C NMR spectra were recorded with a Varian Inova 400 spectrometer operating at 399.92 and 100.57 MHz, respectively, with deuterated chloroform ($CDCl_3$) as the solvent.

UV/vis spectra were recorded using a Hitachi U-3900 UV/vis spectrophotometer.

Accepted manuscrip. Published manuscrip link:
http://www.sciencedirect.com/science/article/pii/S0925400515306948
doi:10.1016/j.snb.2015.11.116

Infrared spectra (FT-IR) were recorded with a FT/IR-4200 FT-IR Jasco spectrometer with an ATR-PRO410-S single reflection accessory. Low-resolution electron impact mass spectra (EI-LRMS) were obtained at 70 eV on an Agilent 6890N mass spectrometer. Thermogravimetric analysis (TGA) data were recorded for a 5-mg sample under a nitrogen or oxygen atmosphere on a TA Instrument Q50 TGA analyser at a scan rate of 10ºC min^{-1}. The limiting oxygen index (LOI) was estimated using the following experimental Van Krevelen equation: LOI = 17.5 + 0.4 CR, where CR is the char yield weight percentage at 800ºC, which was obtained from the TGA measurements under a nitrogen atmosphere.

The water-swelling percentage (WSP) of the membrane was obtained from the weights of a dry sample membrane (ω_d) and a water-swelled sample membrane (ω_s) as follows: 100 x $[(\omega_s-\omega_d)/\omega_d]$ (the membrane was immersed in pure water at 20ºC until the swelled equilibrium was achieved).

To determine the tensile properties of the polymer films (membranes), strips (5 mm in width and 30 mm in length) were cut from polymer films of 112 and 115µm thickness for **Mem1** and **Mem2**, respectively, on a SHIMADZU EZ Test Compact Table-Top Universal Tester at 20ºC. Mechanical clamps were used and an extension rate of 5 mm min^{-1} was applied using a gauge length of 9.44 mm. At least 6 samples were tested for each polymer, and the data was then averaged**.**

The limit of detection (LOD) and limit of quantification were estimated by the following equations: LOD = 3.3 x SD/s and LOQ = 10 x SD/s, where SD is the standard deviation of a blank sample and s is the slope of the calibration curve in a region of low concentration of target species.

Accepted manuscrip. Published manuscrip link:
http://www.sciencedirect.com/science/article/pii/S0925400515306948
doi:10.1016/j.snb.2015.11.116

The qualitative and quantitative chromogenic responses of sensory squares (~5x5 mm) cut from membranes (**Mem1** and **Mem2**) toward Fe(III), Co(II), Cu(II) and Sn(II) in water solution were studied by immersing the squares in a number of sealed vials with 1 mL of buffered water, containing each vial a known concentration of one of the target cations (pH = 2, buffer: KCl-HCl). The resident time was 24 hours and the temperature 25 °C. The qualitative evaluation of the sensing performance of the materials was carried out visually. On the other hand, the quantitative study was performed using a digital picture of the sensory squares taken with a smartphone by treatment of the colour definition data of each disc (RGB parameters, R = purple, G = green, B = blue). These parameters were obtained for each square directly after taking the photograph of the set squares through using the app called ColourMeter of a conventional Android smartphone (for each square 121 (11 × 11) pixels were averaged). The three RGB parameters were reduced to one variable (PC1, principal component 1), using principal component analysis (PCA), which provided an account of >78% of the information on the three RGB parameters, thus allowing for the elaboration of simple 2D titration curves ([cation] vs. PC1) with concomitant noise reduction, without a significant loss of information, and with independence of the type of camera, lighting, quality of the image and so on [31,32].

2.3. Synthesis of sensory monomer

The sensory monomer containing the tpy-motif (**5**) was prepared according with the procedure schematically shown in Scheme 1.

Scheme 1.

Accepted manuscrip. Published manuscrip link:
http://www.sciencedirect.com/science/article/pii/S0925400515306948
doi:10.1016/j.snb.2015.11.116

Synthesis of 3-(4-nitrophenyl)-1-(pyridine-2-yl)prop-2-en-1-one **(1).** 2.5 mL of an aqueous solution of 10% NaOH was added to a suspension of 6.25 g (41.4 mmol) of 4-nitrobenzaldehyde in 50 mL of ethanol. To the resulting mixture cooled at 0 ºC, 5.0 g (41.2 mmol) of 2-acetylpyridine was added dropwise for 3 h. The solution was stirred at 0 ºC for 2 h. The precipitate formed was collected by filtration and washed with ethanol. Yield 6.91 g (66%). ^{1}H NMR δ_H (400 MHz, $CDCl_3$, Me_4Si): 8.75 (1H, d, *J* 4.7 Hz, pyridyl-H); 8.42 (1H, d, *J* 16.1 Hz, CH=CH); 8.26 (2H, d, *J* 8.8 Hz, Ph); 8.19 (1H, d, *J* 7.9 Hz, pyridyl-H); 7.91 (1H, d, *J* 16.1 Hz, CH=CH); 7.90 (1H, td, *J* 7.7 Hz, 1.7 Hz, pyridyl-H); 7.85 (2H, d, *J* 8.9 Hz, Ph); 7.52 (1H,ddd, *J* 7.5 Hz, 4.7 Hz, 1.2 Hz, pyridyl-H). ^{13}C NMR, δ_C (100.6 MHz, $CDCl_3$, Me_4Si): 189.06, 153.73, 149.11, 148.67, 141.44, 141.36, 137.32, 129.36, 127.46, 124.94, 124.25, 123.20. EI-LRMS (m/z (%)): 255.07 (18), 254.07 (M^+, 100), 226.07 (23), 225.06 (68), 180.07 (18), 179.07 (31), 130.04 (16), 102.04 (29), 79.03 (19), 78.03 (20). FTIR [Wavenumbers (cm^{-1})]: $\nu_{ar\ C-H}$: 3075; $\nu_{C=O}$: 1671; $\nu_{C=N}$: 1578; $\nu_{as\ NO_2}$: 1511; $\nu_{s\ NO_2}$: 1334.

Synthesis of 1-pyridylacylpyridinium iodide **(2).** To a solution of 2 g (15.6 mmol) of 2-acetylpyridine in 20 mL of pyridine 4.60 g (17.6 mmol) of I_2 was added and heated at 100 ºC under N_2 atmosphere for 3 h. The mixture was then cooled at room temperature and filtered off and washed with ether. The dry solid was then washed with ethanol. A black solid was obtained. It was immediately used in the next synthetic step because it is sensitive to ambient conditions. Yield 4.03 g (75%). ^{1}H NMR δ_H (300 MHz, $CDCl_3$, Me_4Si): 8.75 (1H, d, *J* 4.7 Hz, pyridyl-H); 8.42 (1H, d, *J* 16.1 Hz, CH=CH); 8.26 (2H, d, *J* 8.8 Hz, Ph); 8.19 (1H, d, *J* 7.9 Hz, pyridyl-H); 7.91 (1H, d, *J* 16.1 Hz, CH=CH); 7.90 (1H, td, *J* 7.7 Hz, 1.7 Hz, pyridyl-H); 7.85 (2H, d, *J* 8.9 Hz, Ph); 7.52 (1H, ddd, *J* 7.5 Hz, 4.7 Hz, 1.2 Hz).

Accepted manuscrip. Published manuscrip link:
http://www.sciencedirect.com/science/article/pii/S0925400515306948
doi:10.1016/j.snb.2015.11.116

***Synthesis of 2-(4-(4-nitrophenyl)-6-(pyridin-2-yl)pyridin-2-yl)pyridine* (3).** To a solution of 10% dry ammonium acetate in 20 mL of ethanol, 1 g (3 mmol) of (**2**) and 0.78 g (3 mmol) (**1**) were added. The mixture was refluxed for two days, the solvent removed and the product used without further purification. Yield 1.00 g (93%). ^{1}H NMR δ_H (400 MHz, $CDCl_3$, Me_4Si): 8.75 (2H, pyridyl-H); 8.73 (2H, d, *J* 4.3 Hz, pyridyl-H); 8.68 (2H, d, *J* 8.0 Hz, pyridyl-H); 8.36 (2H, d, *J* 8.8 Hz, Ph); 8.04 (2H, d, *J* 8.8 Hz, Ph); 7.90 (2H, td, *J* 7.8 Hz, 1.6 Hz, pyridyl-H); 7.38 (2H, pyridyl-H). ^{13}C NMR, δ_C (100.6 MHz, $CDCl_3$, Me_4Si):156.53, 155.81, 149.35, 148.33, 148.02, 145.12, 137.17, 128.43, 124.34, 124.34, 121.56, 119.07. EI-LRMS (m/z (%)):355.11 (25), 354.11 (M^+, 100), 309.12 (20), 308.12 (78), 306.09 (9), 229.07 (57), 203.06 (4), 177.05 (4), 153.54 (5), 78.02 (5). FTIR [Wavenumbers (cm^{-1})]: $\nu_{C=N}$: 1585; $\nu_{as\ NO_2}$: 1514; $\nu_{s\ NO_2}$: 1351.

***Synthesis of 4-(2,6-di(pyridin-2-yl)pyridin-4-yl)benzenamine* (4).** A mixture of 3.66 g (10.3 mmol) of (**3**) and 12.24 g (64.5 mmol) of anhydrous tin(II) chloride in concentrated hydrochloric acid (100 mL) was heated at 70 °C for 6 h. The solid was filtered off and stirred in a 10% aqueous solution of sodium hydroxide for 1 hour. Then it was filtered off and washed with water. Yield 3.07 g (92%). ^{1}H NMR δ_H (400 MHz, $CDCl_3$, Me_4Si): 8.73 (2H, ddd, *J* 4.8 Hz, 1.8 Hz, 0.9 Hz, pyridyl-H); 8.69 (2H, s, pyridyl-H); 8.67 (2H, dt, *J* 8.0 Hz, 1.1 Hz, pyridyl-H); 7.87 (2H, td, *J* 7.7 Hz, 1.8 Hz pyridyl-H); 7.78 (2H, d, *J* 8.5 Hz, Ph); 7.35 (2H, ddd, *J* 7.5 Hz, 4.8 Hz, 1.2 Hz, pyridyl-H); 3.87 (2H, s, NH_2). ^{13}C NMR, δ_C (100.6 MHz, $CDCl_3$, Me_4Si):156.70, 155.88, 150.14, 149.22, 147.67, 136.95, 128.53, 128.38, 123.81, 121.49, 117.93, 115.37. EI-LRMS (m/z (%)):325.13 (24), 324.13 (M^+, 100), 323.12 (19), 296.11 (6), 246.10 (15), 219.09 (6), 162.09 (6), 78 (4). FTIR [Wavenumbers (cm^{-1})]: ν_{NH_2}: 3481, 3387; $\nu_{C=N}$: 1599; δ_{NH_2}: 1338; ν_{C-N}: 1185.

Accepted manuscrip. Published manuscrip link:
http://www.sciencedirect.com/science/article/pii/S0925400515306948
doi:10.1016/j.snb.2015.11.116

***Synthesis of N-(4-(2,4-di(pyridin-2-y)pyridine-4-yl)phenyl)methacrylamide* (5).** A solution of 2.60 g (8 mmol) of (**4**) in 20 mL of NMP was stirred at room temperature for 5 min. Then, 1 g (9.6) mmol of methacryloyl chloride was added dropwise for 20 min. After that, 1.05 g (10.4 mmol) of TEA was added and the mixture is stirred for 4 hs at 50 ºC under nitrogen atmosphere. The solution thus formed was precipitated in water, the solid filtered off and washed with water. Yield 3.07 g (98%). ^{1}H NMR δ_H (400 MHz, $CDCl_3$, Me_4Si): 8.73 (2H, d, *J* 4.3 Hz, pyridyl-H); 8.72 (2H, s, pyridyl-H); 8.66 (2H, d, *J* 8.0 Hz, pyridyl-H); 7.91 (2H, d, *J* 8.7 Hz, Ph); 7.87 (2H, td, *J* 7.8 Hz, 1.6 Hz, pyridyl-H); 7.73 (2H, d, *J* 8.7 Hz, Ph); 7.68 (1H, s, NH); 7.35 (2H,m, pyridyl-H); 5.83 (1H, s, $=CH_2$), 5.49 (1H, s, $=CH_2$), 2.09 (3H, s, CH_3). ^{13}C NMR, δ_C (100.6 MHz, $CDCl_3$, Me_4Si): 171.38, 166.68, 156.40, 156.08, 149.55, 149.25, 141.00, 138.86, 137.01, 134.35, 128.12, 123.96, 121.52, 120.26, 118.55, 18.91. EI-LRMS (m/z (%)): 393.17 (29), 392.16 (M^+, 100), 391.14 (23), 337.14 (6), 351.12 (5), 323.13 (6), 233.09 (19), 78.02 (21), 62.99 (18). FTIR [Wavenumbers (cm^{-1})]: ν_{N-H}: 3301; $\nu_{C=O}$: 1665; $\nu_{C=N}$: 1585; δ_{N-H}: 1519.

2.4. Polymer synthesis

The linear copolymer (**LCp**) was prepared by thermically initiated radical polymerization of the hydrophilic monomer **VP** and the tpy-derivative monomer (**5**) in a 99/1 (**VP**/(**5**)) molar ratio (Scheme 2). A 100-mL three-necked flask equipped with a magnetic stirrer, a nitrogen inlet, and a reflux condenser was charged with a solution of 0.18 mmol (0.071 g) of (**5**) and 17.9 mmol (2.0 g) of **VP** in 18 mL of dioxane. Subsequently, AIBN (0.29 g, 1.8 mmol) was added, and the solution was heated to 60 ºC. After stirring for 4 h under nitrogen, the solution was allowed to cool. The, it was poured dropwise to hexane (200 mL) with vigorous stirring, yielding a white precipitate

Accepted manuscrip. Published manuscrip link:
http://www.sciencedirect.com/science/article/pii/S0925400515306948
doi:10.1016/j.snb.2015.11.116

(Yield 1.61 g (79%)). From the green chemistry viewpoint, the preparation of one gram of polymer **LCp** requires: a) reagents: 15 mg of TEA, 14 mg of methacryloyl chloride, 1.2 mL of HCl_{conc}, 147 mg of $SnCl_2$, 88 mg of ammonium acetate, 46 mg of 2-acetylpyridine, 51 mg of I_2, 31 mg of 4-nitrobenzaldehyde, 240 mg of NaOH, 1.24 g of **VP**, and 180 mg of AIBN; b) solvents: 286 μL of NMP, 1.4 mL of ethanol, 218 μL of pyridine, 212 μL of ether, 11.2 mL of dioxane, and 124.2 mL of hexane.

Scheme 2.

The film-shaped sensory membranes were prepared by the bulk radical polymerization of the hydrophilic monomer **VP**, the hydrophobic monomer **MMA**, and the tpy-containg monomer (**5**). **EGDMMA** was used as cross-linking agent (Scheme 3). The co-monomer molar ratio **VP**/**MMA**/**5**/**EGDMMA** was 50/49.5/0.5/1 and 49/49/2/1 for **Mem1** and **Mem2**, respectively. AIBN (1 wt%) was employed as a thermal radical initiator. The bulk radical polymerization reaction was carried out in a silanized glass mould that was 100 mm thick in an oxygen-free atmosphere at 60 ºC overnight. From the green chemistry viewpoint, the preparation of one gram of membrane requires: a) **Mem1**: reagents (6 mg of TEA, 6 mg of methacryloyl chloride, 487 μL of HCl_{conc}, 51 mg of $SnCl_2$, 35 mg of ammonium acetate, 18 mg of 2-acetylpyridine, 20 mg of I_2, 12 mg of 4-nitrobenzaldehyde, 101 mg of NaOH, 502 mg of **VP**, 452 mg of **MMA**, 18 mg of **EGDMMA**, and 9 mg of AIBN) and solvents (116 μL of NMP, 580 μL of ethanol 88 μL of pyridine, 88 μL of ether); b) **Mem2**: reagents (23 mg of TEA, 22 mg of methacryloyl chloride, 1.9 mL of HCl_{conc}, 228 mg of $SnCl_2$, 136 mg of ammonium acetate, 71 mg of 2-acetylpyridine, 77 mg of I_2, 47 mg of 4-nitrobenzaldehyde, 387 mg of NaOH, 476 mg of **VP**, 428 mg of **MMA**, 17 mg of **EGDMMA**, and 9 mg of AIBN)

Accepted manuscrip. Published manuscrip link:
http://www.sciencedirect.com/science/article/pii/S0925400515306948
doi:10.1016/j.snb.2015.11.116

and solvents (443 μL of NMP, 2.2 mL of ethanol, 337 μL of pyridine, and 337 μL of ether).

Scheme 3.

2.5. Solid sensory substrates

The solid sensory substrates were manufactured form **Mem1** and **Mem2** films by using plastic scissors to cut out 5x5 mm sensory squares. Plastic scissors were used to avoid the presence of iron. Conventional steel scissors turned the membrane coloured (the solely contact of an iron containing object with the membrane surface turns it purple in colour).

3. RESULTS AND DISCUSSION

3.1. Sensing target cations in pure water

The objective of this work is the exploitation of organic molecules in pure water. Organic molecules are usually highly hydrophobic and water insoluble. Their properties in this medium are unknown although they can be envisaged by studying the molecules in organic/aqueous mixtures. Accordingly, an interesting molecule was chosen, its structure was slightly modified by including a polymerizable group, and hydrophilic polymers were prepared. The polymers are both linear (soluble in water), and crosslinked membranes (with gel behaviour as manageable solid kits). With these materials the goal of exploiting water insoluble molecules in pure water was achieved.

3.2. Design of the colorimetric chemosensory terpyridine unit

Firstly metal cations and water as target species and measuring medium, respectively, were selected. A chromogenic response as transduction of the recognition phenomena was also chosen. This is because sensory materials to be used as sensory devices for

Accepted manuscrip. Published manuscrip link:
http://www.sciencedirect.com/science/article/pii/S0925400515306948
doi:10.1016/j.snb.2015.11.116

non-specialized personnel are sought, and the naked eye is the best antenna for this purpose. For meeting this criteria, a proven multivalent chelanting ligand, terpyridine, was chose, which was isolated in 1932 [1], as a guarantee of success [5-19]. Thus, a tpy derivative containing an amine group was used to prepare the acrylamide monomer (**5**), which was co-polymerized with the hydrophilic **VP** and the hydrophobic **MMA** co-monomers.

3.3. Materials preparation and characterisation

The acrylamide sensory monomer (**5**) was conventionally prepared by the straightforward reaction of methacryloyl chloride with the amine group of the intermediate containing the tpy motif (**4**). The preparation of (**4**) was previously reported, and the steps followed to prepare products (**1**) to (**4**) have been adapted from those described by a number of authors looking for inexpensiveness of the chemicals, optimization of the reaction steps, higher reaction yields, easy or no further purification of products [33-37]. The ^{1}H and ^{13}C NMR and FTIR data and the spectra of the intermediates and monomers can be found in the experimental section and in the ESI, Section S1. The potential applicability of the designed acrylic soluble polymer **LCp** and sensory membranes, **Mem1** and **Mem2**, is highlighted by the fact that a small quantity (≤6.8% (**Mem2**), ≤1.8% (**Mem1**)) by weight of the sensory synthetic monomer is used in the preparation of the sensory materials, as will be described below, using (≥93.1% (**Mem2**), ≥98.2% (**Mem1**)) by weight of widely available and very inexpensive commercial co-monomers.

The mechanical and thermal behaviour are key parameters of every material. The membranes, or films, have good physical appearance and were creasable and handleable. Mechanically, they had tensile strength and moduli ranging 33-39 and 660-

Accepted manuscrip. Published manuscrip link:
http://www.sciencedirect.com/science/article/pii/S0925400515306948
doi:10.1016/j.snb.2015.11.116

730 MPa, respectively (Table 1). These results are excellent for lab-made acrylic membranes. The thermal resistance was evaluated using TGA. The degradation temperatures that resulted in a 5% weight loss under a nitrogen atmosphere (T_5) were ~240ºC for membranes and much higher, ~390ºC, for **LCp**. The ester content of the membranes, from the **MMA** co-monomer, lowered the thermal resistance compared with **LCp**. The methyl ester moieties are hydrophobic and counterbalance the hydrophilic nature of **VP** in the membranes in order to control the water-swelling percentage (WSP). Gel behaviour is relevant for the membrane to sense in pure water because the target species enter into the material as solvated species by diffusion. However, the water uptake has to be modulated in order to keep good mechanical properties in the swelled state. For this purpose, a moderate WSP around 40% is desirable. The membranes constitution was designed to meet this criterion. Accordingly, WSP of **Mem1** and **Mem2** was 48% and 36 %, respectively. The hydrophobic nature of the tpy motifs is the responsible of the 12% water uptake decrease upon increasing 1.5% the monomer containing the tpy groups (**5**) (Scheme 3).

Table 1.

3.4. The chemosensing mechanism

The chemosensing mechanism can be described as the coordination of the cation species to the tpy motifs [38]. Thus, the complexation processes of one cation (*M*) and two tpy motifs (*L*) in water. The complex stoichiometry was estimated with a Job´s plot obtained from the UV/vis titration of Fe(III) with water solutions of the sensory polymer **LCp** (Figure 1). The process is governed by two stability constants K_1 and K_2,

$$M + L \overset{K_1}{\rightleftharpoons} ML$$

$$ML + L \overset{K_2}{\rightleftharpoons} ML_2$$

Accepted manuscrip. Published manuscrip link:
http://www.sciencedirect.com/science/article/pii/S0925400515306948
doi:10.1016/j.snb.2015.11.116

where L is the moles of sensory tpy-motifs per water volume of linear copolymer, L represents really not a conventional concentration because the sensory motifs are chemically anchored to the linear copolymer chains. The formation of ML and ML_2 is clearly depicted in the UV/vis titration spectra (Figure 1).

Considering the stability constants definition, the UV/vis spectroscopic data, and the mass balance ($C_M = [M] + [ML] + [ML_2]$; $C_L = [L] + [ML] + 2[ML_2]$), the stability constants can be calculated by non-linear curve fit of Eq. (1), where A is the absorbance, ε_L is calculated initially by $\varepsilon_L = A_0/C_L$, and ε_{ML_2} at the end with a huge excess of metal by $\varepsilon_{ML_2} = 2A_{final}/C_L$ (at this point $[M] \cong C_M$) [39].

$$A = \frac{-1-K_1[M]+\sqrt{(1+K_1[M])^2+8C_LK_1K_2[M]}}{4K_1K_2[M]}\left(\varepsilon_L + \varepsilon_{ML}K_1[M] + \varepsilon_{ML_2}\frac{-1-K_1[M]+\sqrt{(1+K_1[M])^2+8C_LK_1K_2[M]}}{4}\right) \quad (1)$$

The fitting of Eq. (1) to complexation of iron(III) with **LCp** is shown in Figure 1, giving rise to K_1= 51,000 ± 6,000 and K_2= 2,000 ± 1,000. The determination of K_1 and K_2 for Co(II), Cu(II) and Sn(II) could not be carried out because for each cation ML and ML_2 species absorb in the same UV/vis region.

Figure 1.

3.5. Sensing Fe(III), Co(II), Cu(II) and Sn(II) in aqueous media

The addition of transition metal cations to water solutions of **LCp** give rise to the development of clearly visible and nice colours (purple (Fe(III)), orange (Co(II)), green (Cu(II)) and yellow (Sn(II)) (Figure 2). The UV/vis titration curves are depicted in Figures 3 and 4. The response to Fe(III) and Co(II) is conventional (Figure 3), with LOD and LOQ in the sub-micromolar level (1.3×10^{-7} and 3.9×10^{-7} M for the Fe(III) and

Accepted manuscrip. Published manuscrip link:
http://www.sciencedirect.com/science/article/pii/S0925400515306948
doi:10.1016/j.snb.2015.11.116

$6.4x10^{-8}$ and $1.9x10^{-7}$ M for Co(II)). On the other hand, the response to Cu(II) and Sn(II) was rather complex with LOD and LOQ in the sub milimolar level ($1.3x10^{-5}$ and $3.8x10^{-5}$ M for Cu(II) and $1.4x10^{-5}$ and $4.2x10^{-5}$ M for Sn(II)). Only the low concentration region is shown in Figure 4. Full titration curves and UV/vis titration spectra are shown in Figures S6 to S9, ESI.

Figure 2.

Figure 3.

Figure 4.

Solid sensory materials give similar colours upon entering into contact with the cations (Fe(III), Co(II), Cu(II) and Sn(II)), and the differences between solution an solid state for each cation, shown in Figure 2, correspond to concentration differences and colour perception and digitalization. Thus, these materials permitted the preparation of solid titration kits for the visual detection and quantification of cations. Accordingly, squares cut from **Mem1** allowed for the naked eye study of Fe(III) and Co(II) content by analysing the purple and orange colour development, respectively (Figure 5a). The lower sensitivity of the sensory polymers toward Cu(II) and Sn(II), compared with the sensitivity toward Fe(III) and Co(II), was resolved by increasing the tpy sensory motifs within the membranes. Therefore, **Mem2**, which have a molar tpy content four times higher than **Mem1**, permitted the visual titration of Cu(II) and Sn(II) by following the green and yellow colour development, respectively. The digital colour of pictures of sensory squares (sensory kits) shown in Figures 5a and 5b were used to build titration

Accepted manuscrip. Published manuscrip link:
http://www.sciencedirect.com/science/article/pii/S0925400515306948
doi:10.1016/j.snb.2015.11.116

curves with quantification purposes, as previously described. The titration curve for Fe(III) is shown in Figure 5c (the data and titration curves for Co(II), Cu(II) and Sn(II) are depicted in the ESI, Tables S1-S12 and Figures S10-S13) [31,32].

Figure 5.

3.6. Response time

There are key parameters for sensor performance for real live measurements: reliability, accurateness, environmental inertness, and short response time. The response time was calculated as follows: for **LCp** solutions by UV/vis spectroscopy as the time needed to achieve 99% of the absorbance variation (ESI, Figure S14). This time was 10, 6, 2, and 12 min for Fe(III), Co(II), Cu(II), Sn(II) respectively (cations concentration of $5x10^{-6}$, $5x10^{-5}$, $1x10^{-4}$, $7.5x10^{-4}$ M, respectively). The apparent response time of the sensory films (membranes) was slower because of the diffusion of the species into the membrane, and the sensory squares were left immersed overnight.

3.7. Interference study

The selectivity of the sensory materials as colorimetric transition metal cation sensors was tested in the presence of a broad set of cations (NaCl, KCl, $Cu(NO_3)_2{\cdot}3H_2O$, $Co(NO_3)_2{\cdot}6H_2O$, $Al(NO_3)_2{\cdot}9H_2O$, $Pb(NO_3)_2$, LiCl, $Zn(NO_3)_2{\cdot}6H_2O$, $Mg(NO_3)_2{\cdot}6H_2O$, $Cd(NO_3)_2$, $SnCl_2$ and $Ni(NO_3)_2{\cdot}6H_2O$, $SnCl_2$, $Fe(NO_3)_3{\cdot}9H_2O$, $Cu(NO_3)_2{\cdot}3H_2O$, $Co(NO_3)_2{\cdot}6H_2O$). Thus, a solution of **LCp** in water (pH = 2, buffer: KCl-HCl, concentration of sensory motifs in water was $1x10^{-3}$ M -equivalents of pendant sensory tpy motifs per litre-) with a cocktail of these cations (concentration of each cation = $9.09x10^{-4}$ M) was used in this study. The UV/vis spectra show that the set of cations are true interferents (ESI, Figure S15). This is a cause of the broad chelating effect of tpy

Accepted manuscrip. Published manuscrip link:
http://www.sciencedirect.com/science/article/pii/S0925400515306948
doi:10.1016/j.snb.2015.11.116

motifs. This means that a full range of complexes are formed, though only a few are coloured. Accordingly, real sample can contain these ions at different concentrations and this fact may be a drawback for the identification and quantification of the target cations. However, the target cations can also be evaluated in presence of these interferents by the standard addition procedure. For instance, by adding increasing and known quantities of Fe(III) to the sample containing the cocktail of 13 cations (concentration of each cation = $1x10^{-6}$ M), the Fe(III) concentration calculated was $1.3x10^{-6}$ M, similar to the real content, $1.0x10^{-6}$ M (ESI, Figure S16). Furthermore, the accuracy of the Fe(III) concentration determination was verified by measuring the cation concentration in a sample prepared with tap water from our laboratory spiked with Fe(III), thus emulating a real sample. The titration curve was prepared using tap water (the iron concentration of this tap water, determined by inductively coupled plasma mass spectrometry -ICP-, was about 19.4 ppb). The Fe(III) concentration added to the tap water was $1.5x10^{-6}$ M, and the calculated concentration was $1.4x10^{-6}$ M, in good accordance with the added Fe(III) concentration. In parallel, the standard addition method permitted the calculation of the iron concentration of tap water, giving a result of 20.3 ppb, also in agreement with the concentration calculated by ICP.

3.8. Forensic applications and metal recognition

Iron containing tools leave a small amount of metal upon entering into contact with other surfaces. This is relevant in forensic applications where it is important to detect the imprint of certain objects in hands, like knives. In this sense, Figure 6 and a video shows the shape of a lag screw in a finger after holding it with two fingers. After pressing lag screw with the fingers, the index finger is pressed on a filter paper impregnated with an aqueous solution of **LCp**. The iron particles are oxidized by the

Accepted manuscrip. Published manuscrip link:
http://www.sciencedirect.com/science/article/pii/S0925400515306948
doi:10.1016/j.snb.2015.11.116

oxygen of the air, the sweat and water and recognized by the tpy motifs giving rise to the complex formation with the concomitant purple colour development (see video, ESI).

Moreover, it is possible to know if a tool has iron in its composition by dipping in a water solution of **LCp**. Immediately after immersion, the solution turn purple (see Figure 6 and video, ESI).

Cobalt, a critical raw material [40], can also be analysed in a similar way. Figure 6 and the video (ESI) also shows how a widia drill bit, which has an iron-based shaft with a tungsten carbide (with 6-10% of cobalt) blade at the tip off the drill. After being touched with a finger, the widia blade leave on the filter paper, previously wet with the water solution of **LCp**, its orange imprint surrounded by the purple imprint of the iron holding the widia tip.

Figure 6.

4. CONCLUSIONS

Terpyridine, as a proven chelating agent for monoatomic metallic cations, has been used to prepare colorimetric sensory solid polymers both as water soluble linear polymers and as solid films (membranes). Water solution of the linear polymer turned purple, orange, green or yellow upon being in contact with Fe(III), Co(II), Cu(II) and Sn(II), respectively. The colour development permitted the visual differentiation of the cations and the titration with the UV/vis technique. The limit of detection was sub-micromolar for Fe(III) and Co(II), and micromolar for Cu(II) and Sn(II). In a similar fashion, the solid films have gel behaviour and turn coloured upon immersing in water containing the aforementioned cations. Squares cut from the membranes (5x5 mm) behaved as

Accepted manuscrip. Published manuscrip link:
http://www.sciencedirect.com/science/article/pii/S0925400515306948
doi:10.1016/j.snb.2015.11.116

solid sensory kits from which the cations could be differentiated and their concentration estimated by the naked eye. Pictures taken to the kits permitted the titration using the colour definition of the sensory squares as analytical input. The dynamic range was of five decades (lower concentration = $1x10^{-7}$ M) for Fe(III) and Co(II) and of two decades (lower concentration = $9x10^{-5}$ M) for Cu(II) and Sn(II). The chosen of proven organic chelating agents and their chemical anchorage to polymer backbones have proven to be successful strategies to prepare sensory materials for water environments. The colour output of the sensory systems and the manageable solid kits allowed for the visually use of these materials by non-specialized personnel and, concomitantly, portable devices such as smartphones permit the fast and costless quantification of target species. Moreover, forensic applications are envisaged, e.g., the shape of metallic objects after entering into contact with hands can be colour revealed by pressing the hands on paper or cotton fabrics wetted with water solutions of the linear sensory polymer.

Acknowledgments

The financial support provided by the Spanish Ministerio de Economía y Competitividad-Feder (MAT2014-54137-R) and by the Consejería de Educación – Junta de Castilla y León (BU232U13) is gratefully acknowledged.

Apendix A. Supplementary data

A file and a video. The file containing experimental part (intermediates and monomer characterization); study of interaction of **LCp**, **Mem1** and **Mem2** with Fe(III), Co(II), Cu(II), and Sn(II); interference study; and response time. The video showing the forensic applications and metal recognition of metallic goods with solutions of **LCp**.

Accepted manuscrip. Published manuscrip link:
http://www.sciencedirect.com/science/article/pii/S0925400515306948
doi:10.1016/j.snb.2015.11.116

References

[1] G. T. Morgan, F. H. Burstall, Dehydrogenation of pyridine by anhydrous ferric chloride, J. Chem. Soc. (1932) 20-30.
[2] C. E. Housecroft, 4,2′:6′,4″-Terpyridines: diverging and diverse building blocks in coordination polymers and metallomacrocycles, Dalton Trans. 43 (2014) 6594-6604.
[3]. E. C. Constable, C. E. Housecroft, M. Neuburger, S. Schaffner, L. J. Scherer, Preparation and structural characterisation of terpy-cored dendrimers and dendriplexes, Dalton Trans. (2004) 2635-2642.
[4] P. Wang, T. Okamura, H.-P. Zhou, W.-Y. Sun, Y.-P. Tian, Metal complex with terpyrindine derivative ligand as highly selective colorimetric sensor for iron(III), Chin. Chem. Lett. 24 (2013) 20-22.
[5] B. Zhang, Y. Li, W. Sun, Anion-sensitive 2,4-dinitrophenylhydrazone-containing terpyridine derivative and its platinum chloride complex, Eur. J. Inorg. Chem. (2011) 4964-4969.
[6] C. Bhaumik, D. Maity, S. Das, S. Baitalik, Anion sensing studies of luminescent bis-tridentate ruthenium(II) and osmium(II) complexes based on terpyridyl-imidazole ligand through different channels, Polyhedron 52 (2013) 890-899.
[7] Q.-Y. Cao, M. Li, L. Zhoua, Z.-W. Wang, New 2,2′:6′,2″-terpyridines as colorimetric and fluorescent sensors for fluoride ions, RSC Adv. 4 (2014) 4041–4046.
[8] S. Bhowmik, B. N. Ghosh, V. Marjomäki, K. Rissanen, Nanomolar pyrophosphate detection in water and in a self-assembled hydrogel of a simple terpyridine-Zn^{2+} complex, J. Am. Chem. Soc. 136 (2014) 5543-5546.
[9] A. Fermi, G. Bergamini, M. Roy, M. Gingras, P. Ceroni, Turn-on phosphorescence by metal coordination to a multivalent terpyridine ligand: a new paradigm for luminescent sensors, J. Am. Chem. Soc. 136 (2014) 6395-6400.
[10] C. Goze, G. Ulrich, L. Charbonnière, M. Cesario, T. Prangé, R. Ziessel, Cation sensors based on terpyridine-functionalized boradiazaindacene, Chem. Eur. J. 9 (2003) 3748-3755.
[11] Y. Zhang, C. B. Murphy, W. E. Jones Jr, Poly[*p*-(phenyleneethynylene)-alt-(thienyleneethynylene)] polymers with oligopyridine pendant groups: highly sensitive chemosensors for transition metal ions, Macromolecules 35 (2002) 630-636.
[12] M. A. R. Meier, U. S. Schubert, Fluorescent sensing of transition metal ions based on the encapsulation of dithranol in a polymeric core shell architecture, Chem. Commun. (2005) 4610-4612.
[13] C. Fan, X. Wang, P. Ding, J, Wang, Z, Liang, X, Tao, Synthesis, photophysical and iron-sensing properties of terpyridyl-based triphenylamine derivatives, Dyes Pigm. 95(2012) 757-767.
[14] H. Li, S.-J. Zhang, C.-L. Gong, Y.-F. Li, Y. Liang, Z.-G. Qi, S. Chen, Highly sensitive and selective fluorescent chemosensor for Ni^{2+} based on a new poly(arylene ether) with terpyridine substituent groups, Analyst 138 (2013) 7090-7093.
[15] Y. Hong, S. Chen, C. W. T. Leung, J. W. Y. Lam, J. Liu, N.-W. Tseng, R. T. K. Kwok, Y. Yu, Z. Wang, B. Z. Tang, Fluorogenic Zn(II) and chromogenic Fe(II) sensors based on terpyridine-substituted tetraphenylethenes with aggregation-induced emission characteristics, ACS Appl. Mater. Interfaces 3 (2011) 3411-3418.
[16] M. Zheng, H. Tan, Z. Xie, L. Zhang, X. Jing, Z. Sun, Fast response and high sensitivity europium metal organic framework fluorescent probe with chelating terpyridine sites for Fe^{3+}, ACS Appl. Mater. Interfaces 5 (2013) 1078-1083.
[17] M. E. Padilla-Tosta, J. M. Lloris, R. Martínez-Máñez, A. Benito, J. Soto, T. Pardo, M. A. Miranda, M. D. Marcos, Bis(terpyridyl)-Ruthenium(II) units attached to polyazacycloalkanes as sensing fluorescent receptors for transition metal ions, Eur. J. Inorg. Chem. (2000) 741-748.
[18] Z.-B. Zheng, Z.-M. Duan, J.-X. Zhang, K.-Z. Wang, Chromogenic and fluorogenic sensing properties toward cations and anions by a terpyridine/phenylimidazo [4,5-*f*]phenanthroline hybrid, Sens. Actuators B 169(2012) 312-319.
[19] C. Bhaumik, S. Das, D. Maity, S. Baitalik, A terpyridyl-imidazole (tpy-HImzPh_3) based bifunctional receptor for multichannel detection of Fe^{2+} and F^- ions, Dalton Trans. 40 (2011) 11795-11808.
[20] C. Y.-S. Chung, V. W.-W. Yam, Induced self-assembly and Förster resonance energy transfer studies of alkynylplatinum(II) terpyridine complex through interaction with water-soluble poly(phenylene ethynylene sulfonate) and the proof-of-principle demonstration of this two-

Accepted manuscrip. Published manuscrip link:
http://www.sciencedirect.com/science/article/pii/S0925400515306948
doi:10.1016/j.snb.2015.11.116

component ensemble for selective label-free detection of human serum albumin, J. Am. Chem. Soc. 133 (2011) 18775-18784.
[21] H.-L. Kwong, W.-L. Wonga, C.-S. Lee, C.-T. Yeung, P.-F. Teng, Zinc(II) complex of terpyridine-crown macrocycle: A new motif in fluorescence sensing of zwitterionic amino acids, Inorg. Chem. Commun. 12 (2009) 815-818.
[22] G. N. Tew, K. A. Aamer, R. Shunmugam, Incorporation of terpyridine into the side chain of copolymers to create multi-functional materials, Polymer 46 (2005) 8440-8447.
[23] R. Shunmugam, G. N. Tew, Polym, Dialing in color with rare earth metals: facile photoluminescent production of true white light, Adv. Technol. 18 (2007) 940-950.
[24] Etienne Baranoff, Jean-Paul Collin, Lucia Flamigni, Jean-Pierre Sauvage, From ruthenium(II) to iridium(III): 15 years of triads based on bis-terpyridine complexes, Chem. Soc. Rev. 33 (2004) 147-155.
[25] E. G. Moore, M. Benaglia, G. Bergamini, P. Ceroni, Synthesis, Stability and Sensitised Lanthanide Luminescence of Heterobimetallic d/f Terpyridine Complexes, Eur. J. Inorg. Chem. (2015) 414-420.
[26] S. Caramori, J. Husson, M. Beley, C. A. Bignozzi, R. Argazzi, P. C. Gros, Combination of cobalt and iron polypyridine complexes for improving the charge separation and collection in ru(terpyridine)$_2$-sensitised solar cells, Chem. Eur. J. 16 (2010) 2611-2618.
[27] A. Winter, G. R. Newkome, U. S. Schubert, Catalytic applications of terpyridines and their transition metal complexes, ChemCatChem 3 (2011) 1384-1406.
[28] H. Hofmeier, U. S. Schubert, Recent developments in the supramolecular chemistry of terpyridine–metal complexes, Chem. Soc. Rev. 33 (2004) 373-399.
[29] P. R. Andres, U. S. Schubert, New functional polymers and materials based on 2,2′:6′,2″-terpyridine metal complexes, Adv. Mater. 16 (2004) 1043-1068.
[30] R. shanmugam, G. J. Gabriel, C. E. Smith, D. A. Aamer, G. N. Tew, Highly selective colorimetric aqueous sensor for mercury, Chem. Eur. J. 14 (2008) 3904-3907.
[31] H. El Kaoutit, P. Estevez, F. C. Garcia, F. Serna, J. M. Garcia, Sub-ppm quantification of Hg(II) in aqueous media using both the naked eye and digital information from pictures of a colorimetric sensory polymer membrane taken with the digital camera of a conventional mobile phone, Anal. Methods 5 (2013) 54-58.
[32] S. Vallejos, A. Muñoz, S. Ibeas, F. Serna, F. C. Garcia, J. M. Garcia, Solid sensory polymer substrates for the quantification of iron in blood, wine and water by a scalable RGB technique, J. Mater. Chem. A 1 (2013) 15435-15441.
[33] P. Lainé, F. Bedioui, P. Ochsenbein, V. Marvaud, M. Bonin, E. Amouyal, A new class of functionalized terpyridyl ligands as building blocks for photosensitized supramolecular architectures. synthesis, structural, and electronic characterizations, J. Am. Chem. Soc., 124 (2002) 1364-1377.
[34] F. Tessore, D. Roberto, R. Ugo, M. Pizzotti, Terpyridine Zn(II), Ru(III), and Ir(III) complexes: the relevant role of the nature of the metal ion and of the ancillary ligands on the second-order nonlinear response of terpyridines carrying electron donor or electron acceptor groups, Inorg. Chem.44 (2005) 8967-8978.
[35] E. Zysman-Colman, J. D. Slinker, J. B. Parker, G. G. Malliaras, S. Bernhard, Improved turn-on times of light-emitting electrochemical cells, Chem. Mater. 20 (2008) 388-396.
[36] G. A. Koohmareh, M. Sharifi, Synthesis, characterization, and coordination behavior of copoly(styrene-maleimide) functionalized with terpyridine, J. Appl. Polym. Sci. 116 (2010) 179-183.
[37] W. Y. Ng, X. Gong, W. K. Chan, Electronic and light-emitting properties of some polyimides based on bis(2,2‘:6‘,2‘ ‘-terpyridine) ruthenium(II) complex, Chem. Mater. 11 (1999) 1165-1170.
[38] A. Earnshaw, N. Greenwood, Chemistry of the Elements, 2nd Ed., Elsevier Butterworth-Heinemann, Burlington, 2005, ch 19.
[39] S. Vallejos, P. Estévez, S. Ibeas, F. C. García, F. Serna, J. M. García, An organic/inorganic hybrid membrane as a solid “turn-on” fluorescent chemosensor for coenzyme A (CoA), cysteine (Cys), and glutathione (GSH) in aqueous media, Sensors 12 (2012) 2969-2982.
[40] *Report on critical raw materials for the* EU, Report of the Ad hoc Working Group on defining critical raw materials, European Commission, May 2014. Downloaded: July 14, 2015 (http://ec.europa.eu/enterprise/policies/raw-materials/files/docs/crm-report-on-critical-raw-materials_en.pdf).

Tables

Table 1. Thermal (TGA) and mechanical properties of materials. The thermal properties were evaluated in inert (N_2) and oxidizing (synthetic air) atmospheres.

Polymer	Thermal properties						Mechanical properties		
	Atmosphere								
	N_2			Air		LOI[c]	Tensile strength, MPa	Young's Modulus, MPa	Elongation, %
	T_5,[a] °C	T_{10},[a] °C	CR,[b] %	T_5,[a] °C	T_{10},[a] °C				
Mem1	242	344	4	224	318	19.1	33	660	9
Mem2	241	342	4	245	333	19.1	39	730	8
LCp	389	408	1	353	399	17.9	n.a.[d]	n.a.[d]	n.a.[d]

[a] 5% weight loss (T_5), 10% weight loss (T_{10}); [b] CR: char yield at 800 ºC; [c] limiting oxygen index, calculated from the TGA data (LOI = 17.5 + 0.4 CR, CR at 800 ºC under nitrogen).[d] n.a.: not applicable.

Captions

Graphical abstract

Films and water soluble polymers as sensory materials for the detection and quantification of iron, cobalt, copper and tin salts in water, and for forensic applications.

Schemes

Scheme 1. Synthesis of acylic monomer (**5**).

Scheme 2. Synthesis and chemical structure of sensory linear polymer (**LCp**).

Scheme 3. Synthesis and chemical structure of sensory membranes **Mem1** and **Mem2**. The picture shows the membranes after removal from the mould.

Figures

Figure 1. UV/vis study of the interaction of Fe(III) (*M*) with tpy-motif (*L*) of **LCp** in water (pH = 2, buffer = HCl-KCl): a) absorbance variation spectra. Blue and red spectra correspond to formation of 1:1 (*ML*) and 1:2 (ML_2) complexes tpy motif:Fe(III), respectively (inset: separation of processes with indication of the isosbestic points); b) absorbance at 567 nm vs Fe(III) concentration. The continuous line is the fitting of the data according with Eq. (1) (inset: Job´s plot (χ_{tpy} is molar fraction of tpy sensory motifs, absorbance at 567 nm); and c) the species distribution. The concentration of sensory motifs in water was $1x10^{-4}$ M (equivalents of pendant sensory tpy motifs per litre).

Figure 2. Colour development sensory materials upon entering into contact with Fe(III), Co(II), Cu(II) and Sn(II): a) **LCp** in water solution (pH = 2, buffer = KCl-HCl, concentration of cations = $5x10^{-4}$ M). The concentration of sensory motifs in water was 0.01 M (equivalents of pendant sensory tpy motifs per litre); and b) **Mem1** after immersion in water (pH = 2, buffer = KCl-HCl, concentration of cations = $5x10^{-4}$ M, immersion time = 24 h).

Figure 3. Titration curves of Fe(III) and Co(II) with aqueous solutions of **LCp** (pH = 2, buffer = KCl-HCl, concentration of cations ranging from $6.75x10^{-8}$ to $6.57x10^{-4}$ M for Fe(III) and $7.99x10^{-8}$ to $7.54x10^{-4}$ M for Co(II). Insets: expansion of the low concentration region. The concentration of sensory motifs in water was $1x10^{-4}$ M for the Fe(III) titration and $1x10^{-3}$ M for the Co(II) titration (equivalents of pendant sensory tpy motifs per litre).

Figure 4. Titration curves of: a) Cu(II); and b) Sn(II) with aqueous solutions of **LCp** (pH = 2, buffer = KCl-HCl, concentration of cations ranging from $1.64x10^{-5}$ to $1.46x10^{-}$

^{3} M for Cu(II) and 3.44x10^{-5} to 1.50x10^{-3} M for Sn(II) M. The concentration of sensory motifs in water was 1x10^{-3} M (equivalents of pendant sensory tpy motifs per litre).

Figure 5. Visual titration of Fe(III), Co(II), Cu(II) and Sn(II) in water (pH = 2, buffer = KCl-HCl) with squares cut from **Mem1** or **Mem2**. Each square was dipped in the water solution containing each cation for 24 h. The sensory membrane and the cation concentration of the water solution was: a) membranes = **Mem1**, Fe(III) and Co(II) concentration, from left to right: 1x10^{-7}, 5x10^{-7}, 1x10^{-6}, 5x10^{-6}, 1x10^{-5}, 5x10^{-5}, 1x10^{-4}, 5x10^{-4}, 1x10^{-3}, 5x10^{-3} M; b) membranes = **Mem2**, Cu(II) and Sn(II) concentration, from left to right: 9x10^{-5}, 3x10^{-4}, 6x10^{-4}, 9x10^{-4}, 3x10^{-3}, 6x10^{-3}, 9x10^{-3} M; and c) Fe(III) titration curve obtained from the picture taken to the squares immersed in water with Fe(III) (PC1: principal component 1 that encompass three digital colour parameters (RGB) of each sensory square).

Figure 6. Detecting iron and cobalt with a water solution of **LCp** (pH = 2, buffer: KCl-HCl, 1.14 mg/mL (concentration of sensory motifs was 1.75x10^{-3} M -equivalents of pendant sensory tpy motifs per litre-)): a) shape of a lag screw in a finger; b) coloration of the **LCp** solution caused by the iron of the lag screw; and c) shape of a widia blade (tungsten carbide + 6-10% of cobalt) of a drill bit.

Graphical abstract

Films and water soluble polymers as sensory materials for the detection and quantification of iron, cobalt, copper and tin salts in water, and for forensic applications.

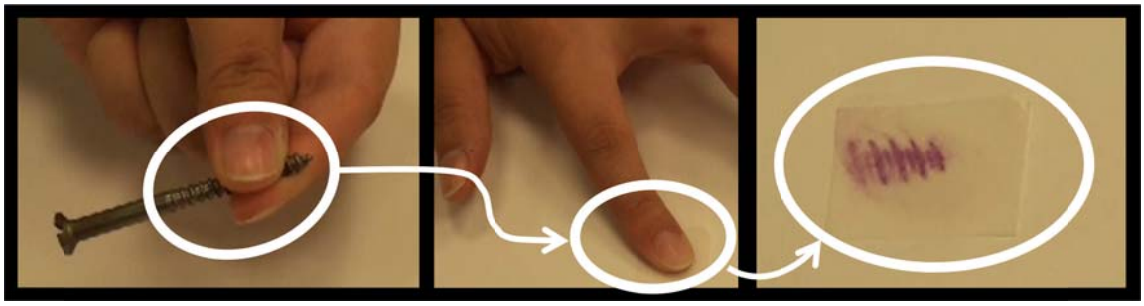

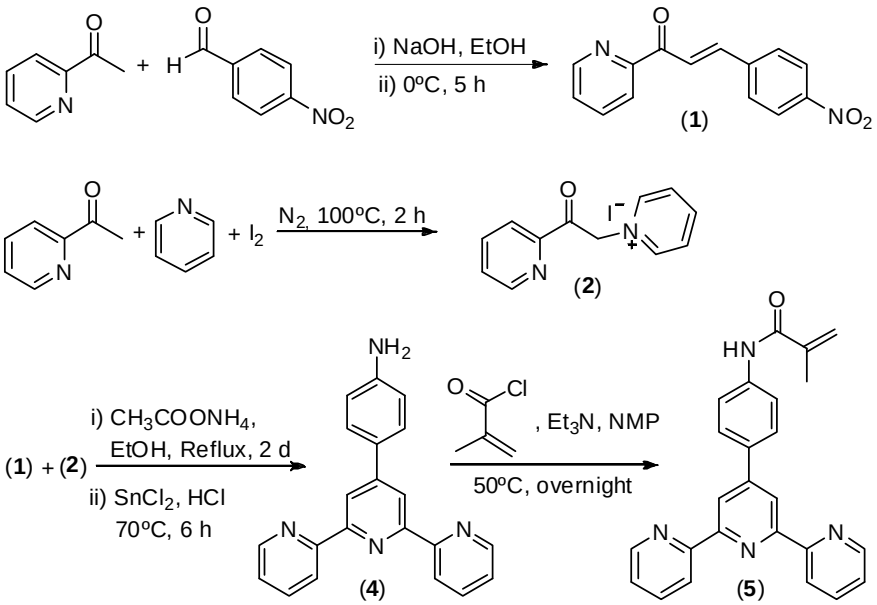

Scheme 1. Synthesis of acylic monomer (**5**).

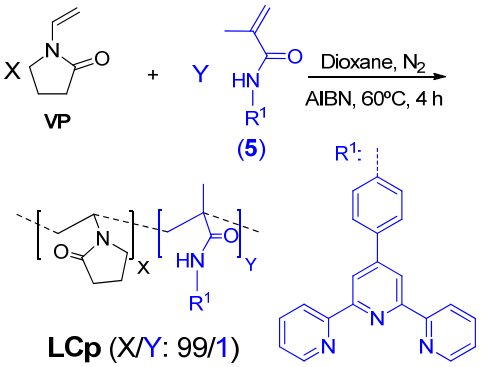

Scheme 2. Synthesis and chemical structure of sensory linear polymer (**LCp**).

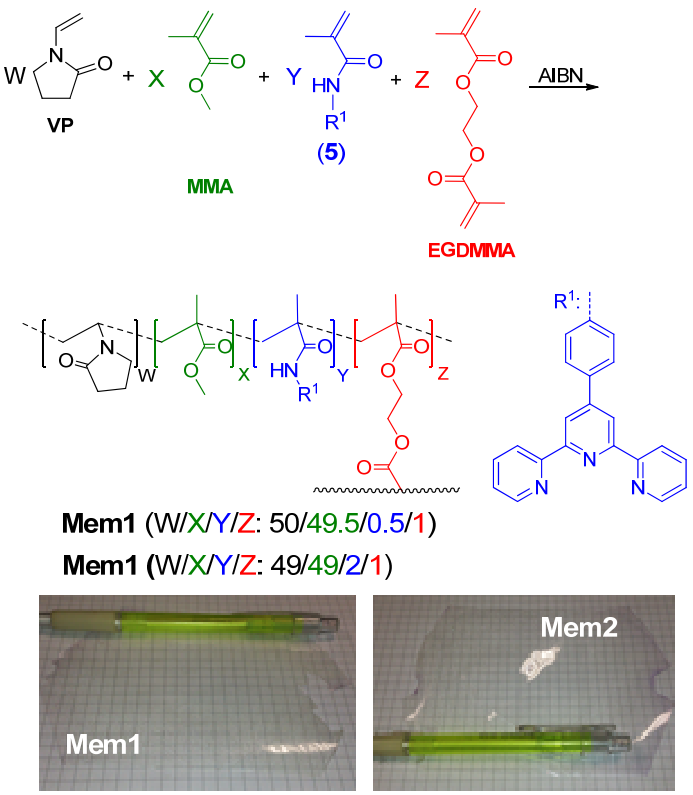

Scheme 3. Synthesis and chemical structure of sensory membranes **Mem1** and **Mem2**. The picture shows the membranes after removal from the mould.

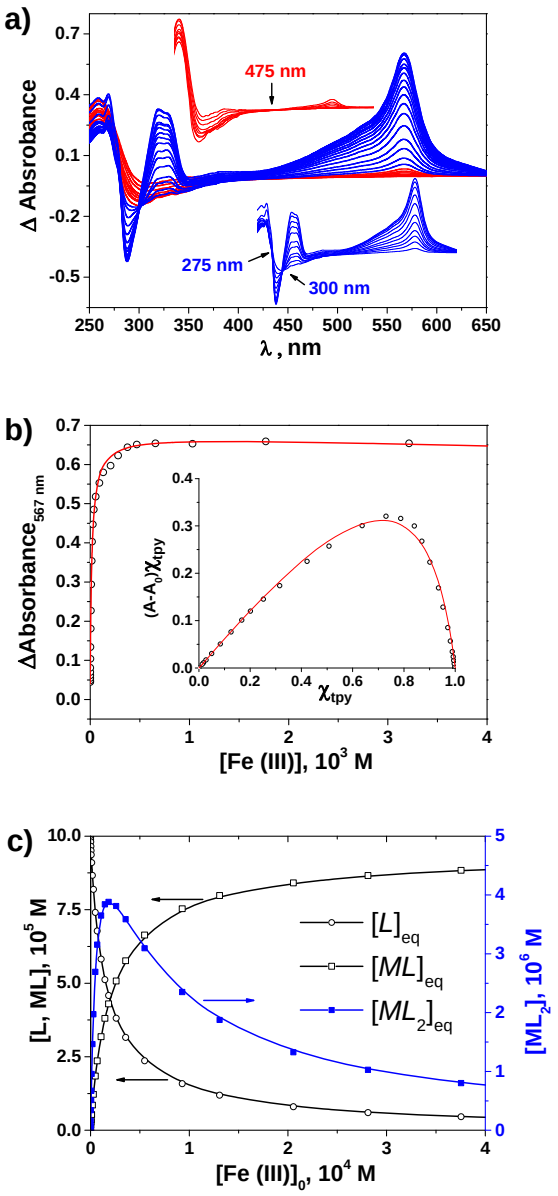

Figure 1. UV/vis study of the interaction of Fe(III) (*M*) with tpy-motif (*L*) of **LCp** in water (pH = 2, buffer = HCl-KCl): a) absorbance variation spectra. Blue and red spectra correspond to formation of 1:1 (*ML*) and 1:2 (ML_2) complexes tpy motif:Fe(III), respectively (inset: separation of processes with indication of the isosbestic points); b) absorbance at 567 nm vs Fe(III) concentration. The continuous line is the fitting of the data according with Eq. (1) (inset: Job´s plot (χ_{tpy} is molar fraction of tpy sensory motifs, absorbance at 567 nm); and c) the species distribution. The concentration of sensory motifs in water was $1x10^{-4}$ M (equivalents of pendant sensory tpy motifs per litre).

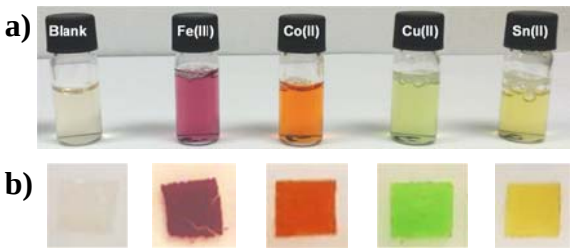

Figure 2. Colour development sensory materials upon entering into contact with Fe(III), Co(II), Cu(II) and Sn(II): a) **LCp** in water solution (pH = 2**,** buffer = KCl-HCl, concentration of cations = $5x10^{-4}$ M). The concentration of sensory motifs in water was 0.01 M (equivalents of pendant sensory tpy motifs per litre**)**; and b) **Mem1** after immersion in water (pH = 2, buffer = KCl-HCl, concentration of cations = $5x10^{-4}$ M, immersion time = 24 h).

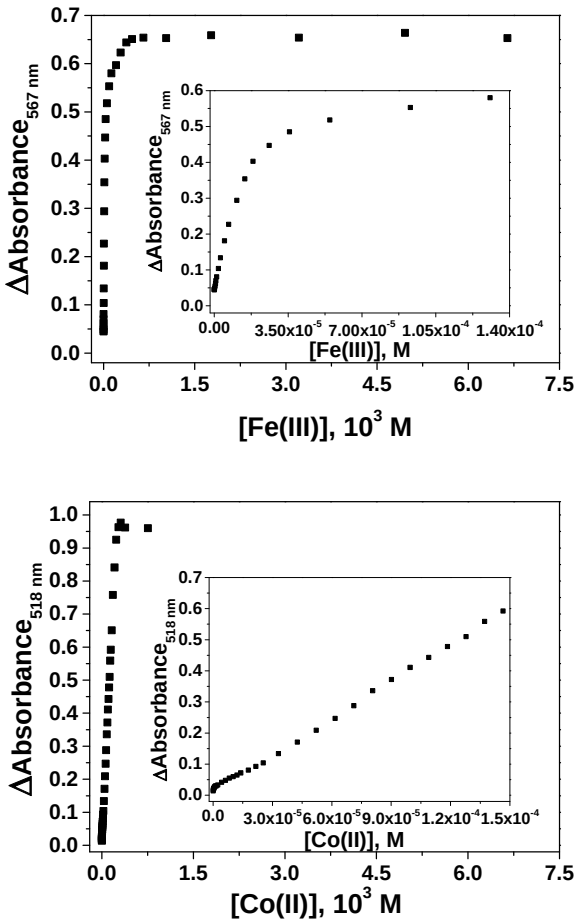

Figure 3. Titration curves of Fe(III) and Co(II) with aqueous solutions of **LCp** (pH = 2, buffer = KCl-HCl, concentration of cations ranging from 6.75×10^{-8} to 6.57×10^{-4} M for Fe(III) and 7.99×10^{-8} to 7.54×10^{-4} M for Co(II). Insets: expansion of the low concentration region. The concentration of sensory motifs in water was 1×10^{-4} M for the Fe(III) titration and 1×10^{-3} M for the Co(II) titration (equivalents of pendant sensory tpy motifs per litre).

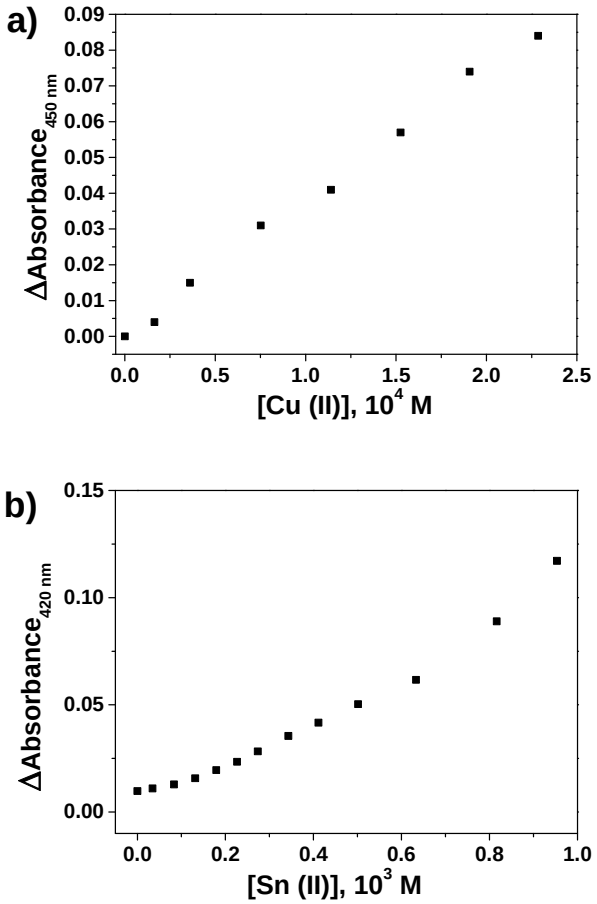

Figure 4. Titration curves of: a) Cu(II); and b) Sn(II) with aqueous solutions of **LCp** (pH = 2, buffer = KCl-HCl, concentration of cations ranging from 1.64×10^{-5} to 1.46×10^{-3} M for Cu(II) and 3.44×10^{-5} to 1.50×10^{-3} M for Sn(II) M. The concentration of sensory motifs in water was 1×10^{-3} M (equivalents of pendant sensory tpy motifs per litre).

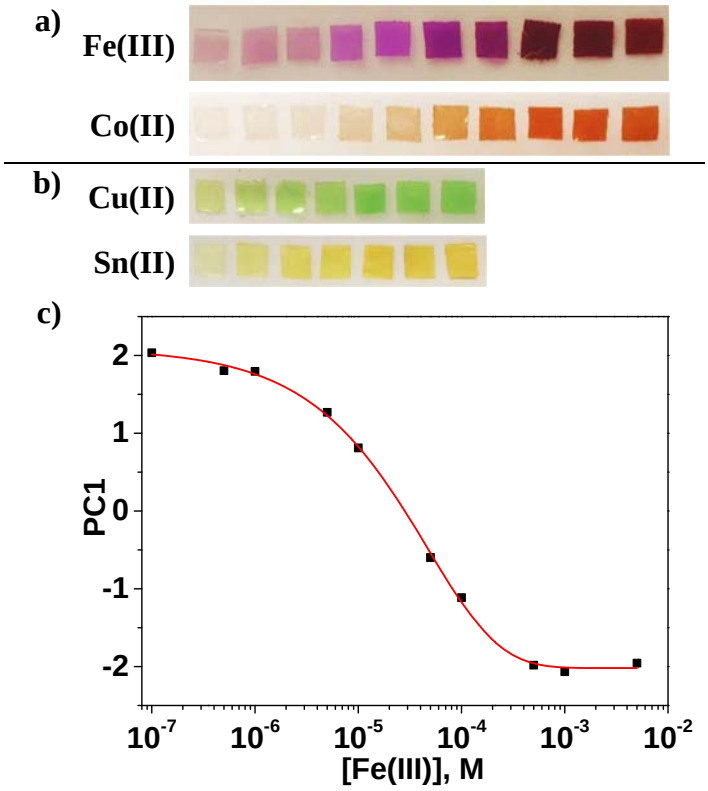

Figure 5. Visual titration of Fe(III), Co(II), Cu(II) and Sn(II) in water (pH = 2, buffer = KCl-HCl) with squares cut from **Mem1** or **Mem2**. Each square was dipped in the water solution containing each cation for 24 h. The sensory membrane and the cation concentration of the water solution was: a) membranes = **Mem1**, Fe(III) and Co(II) concentration, from left to right: $1x10^{-7}$, $5x10^{-7}$, $1x10^{-6}$, $5x10^{-6}$, $1x10^{-5}$, $5x10^{-5}$, $1x10^{-4}$, $5x10^{-4}$, $1x10^{-3}$, $5x10^{-3}$ M; b) membranes = **Mem2**, Cu(II) and Sn(II) concentration, from left to right: $9x10^{-5}$, $3x10^{-4}$, $6x10^{-4}$, $9x10^{-4}$, $3x10^{-3}$, $6x10^{-3}$, $9x10^{-3}$ M; and c) Fe(III) titration curve obtained from the picture taken to the squares immersed in water with Fe(III) (PC1: principal component 1 that encompass three digital colour parameters (RGB) of each sensory square).

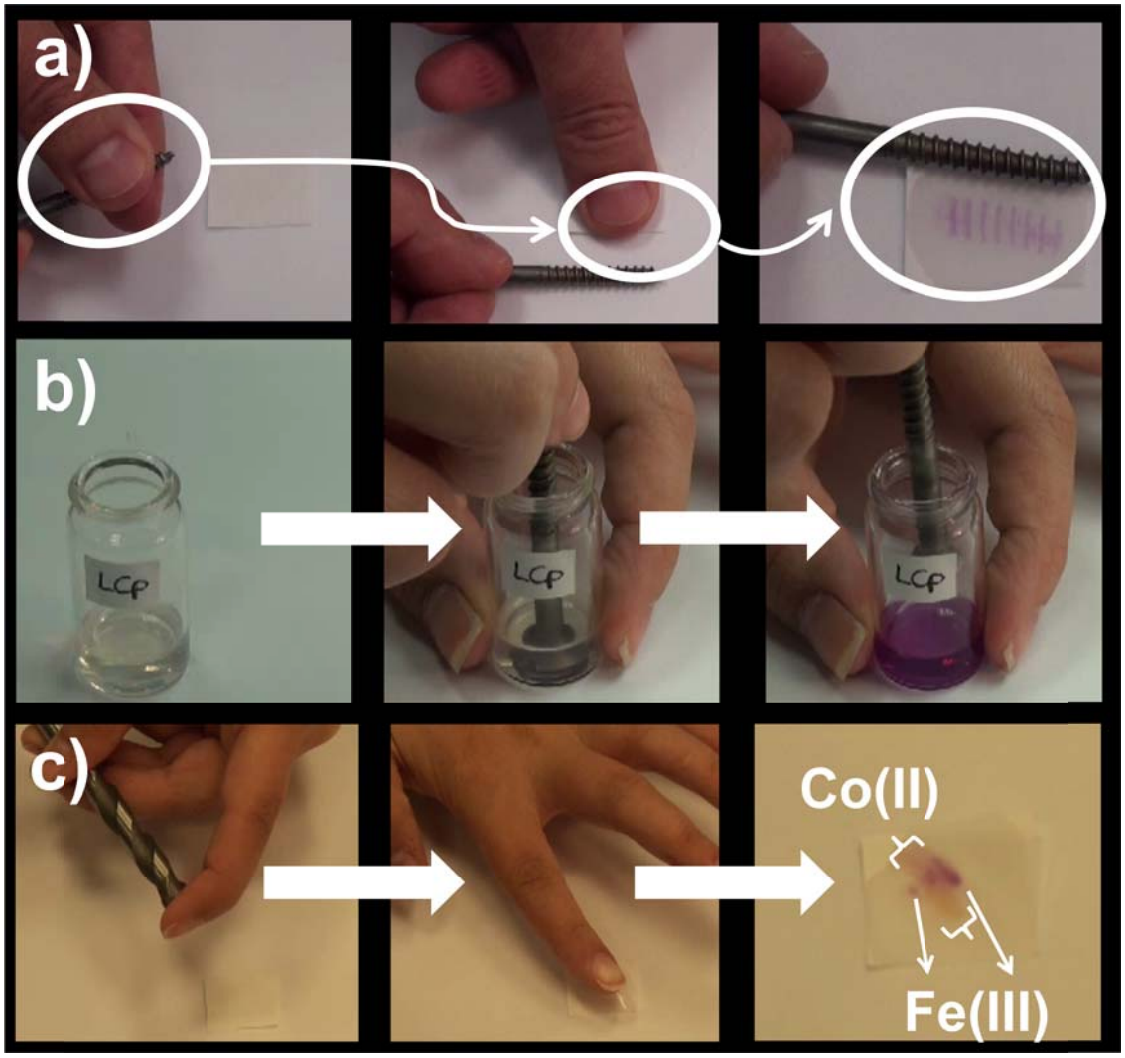

Figure 6. Detecting iron and cobalt with a water solution of **LCp** (pH = 2, buffer: KCl-HCl, 1.14 mg/mL (concentration of sensory motifs was 1.75×10^{-3} M -equivalents of pendant sensory tpy motifs per litre-)): a) shape of a lag screw in a finger; b) coloration of the **LCp** solution caused by the iron of the lag screw; and c) shape of a widia blade (tungsten carbide + 6-10% of cobalt) of a drill bit.

SUPPORTING INFORMATION

Colorimetric detection and determination of Fe(III), Co(II), Cu(II) and Sn(II) in aqueous media by acrylic polymers with pendant terpyridine motifs

Miriam Trigo-López, Asunción Muñoz, Saturnino Ibeas, Felipe Serna, Félix Clemente García and José Miguel García*

Departamento de Química, Facultad de Ciencias, Universidad de Burgos, Plaza de Misael Bañuelos s/n, 09001 Burgos, Spain. Fax: (+) 34 947 258 831, Tel: (+) 34 947 258 085. E-mail: jmiguel@ubu.es

Table of contents

S1. Experimental part. Intermediate and monomer characterisation

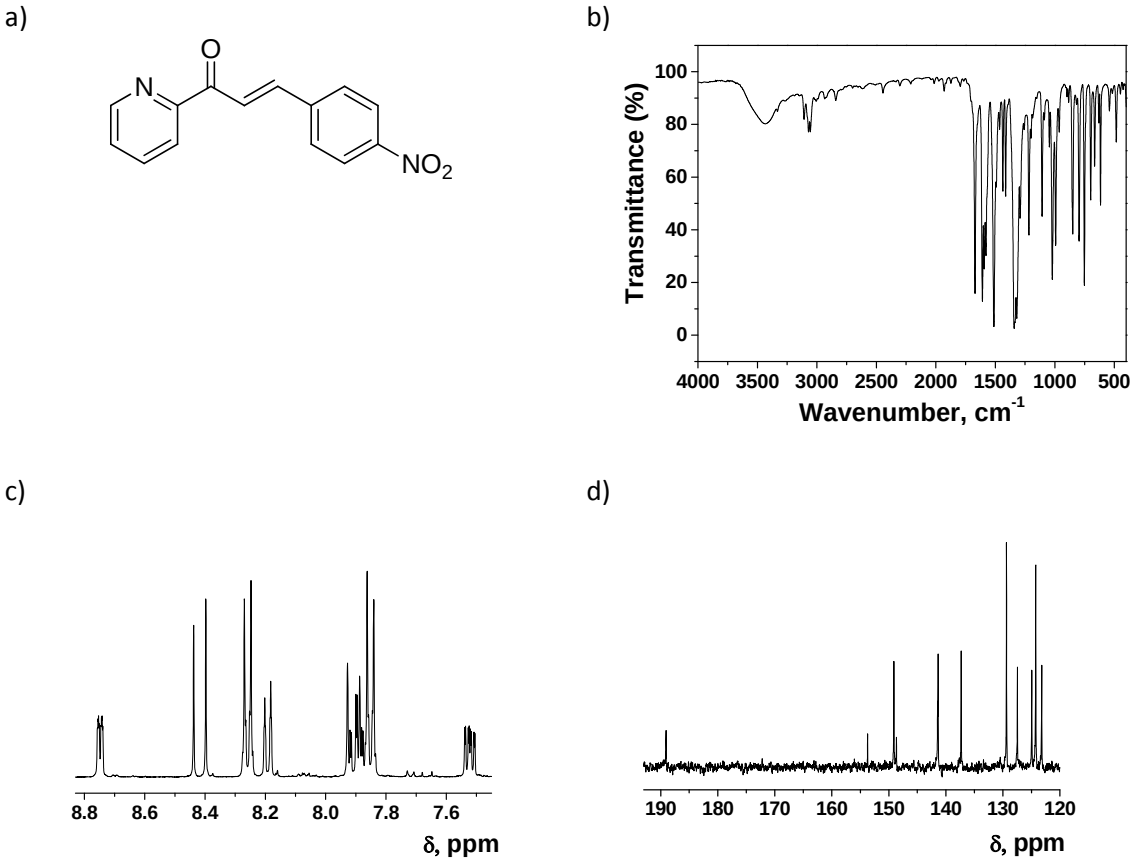

Figure S1. Characterisation of (3-(4-nitrophenyl)-1-(pyridine-2-yl)prop-2-en-1-one (**1**): a) chemical structure; b) FT-IR; c) ^{1}H NMR; d) ^{13}C NMR (NMR solvent: DMSO-d_6).

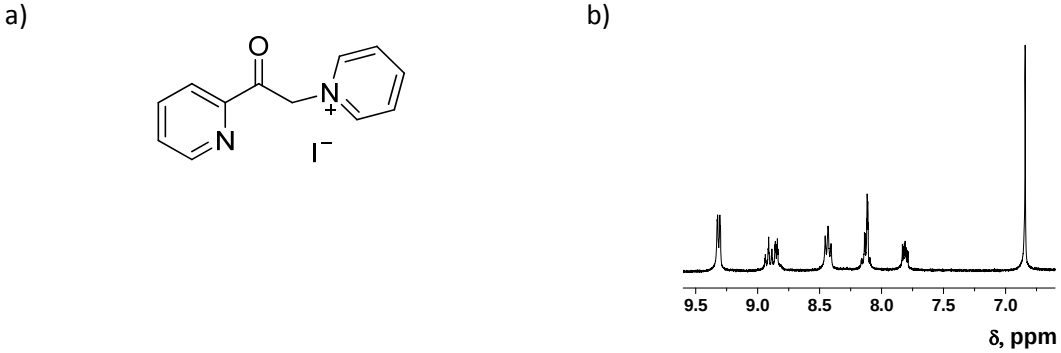

Figure S2. Characterisation of 1-pyridylacylpyridinium iodide (**2**): a) chemical structure; b) ^{1}H NMR (NMR solvent: DMSO-d_6).

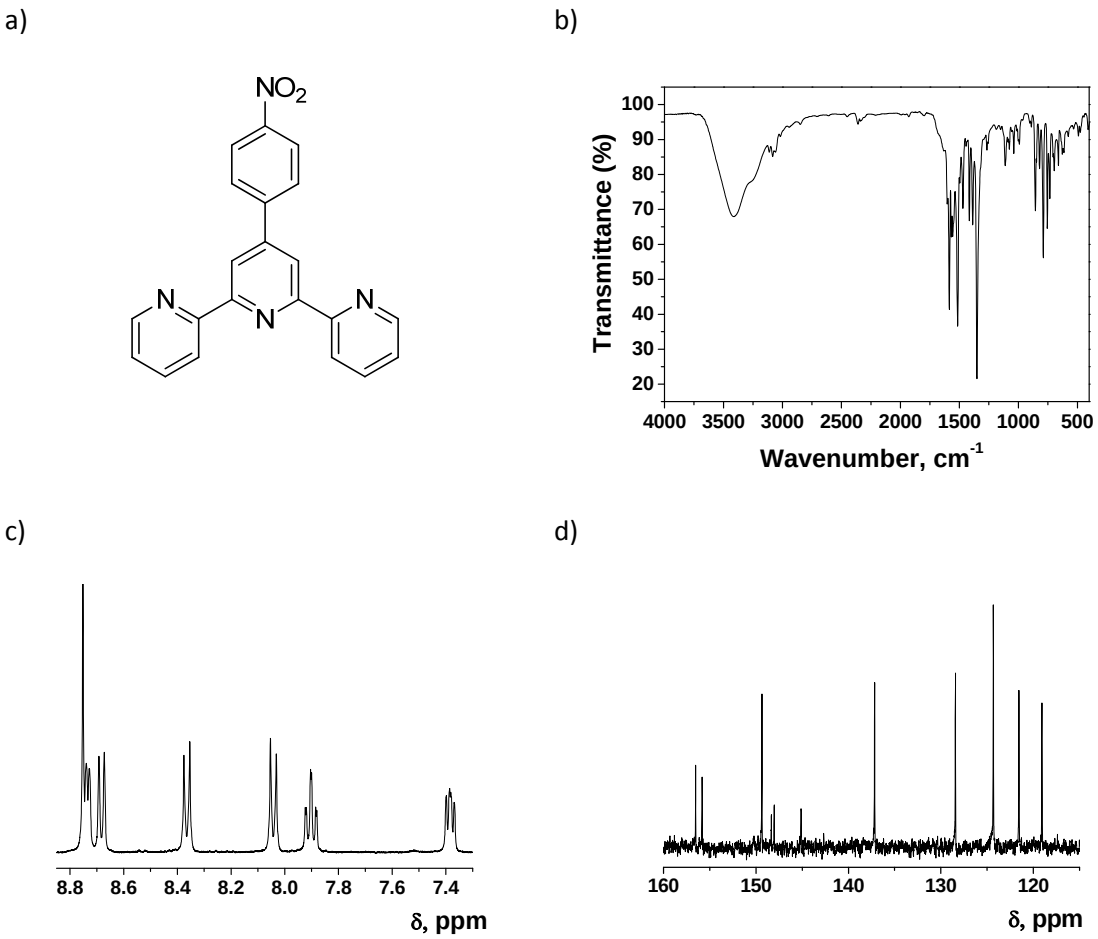

Figure S3. Characterisation of 2-(4-(4-nitrophenyl)-6-(pyridin-2-yl)pyridin-2-yl)pyridine (**3**): a) chemical structure; b) FT-IR; c) ^{1}H NMR; d) ^{13}C NMR (NMR solvent: DMSO-d_6).

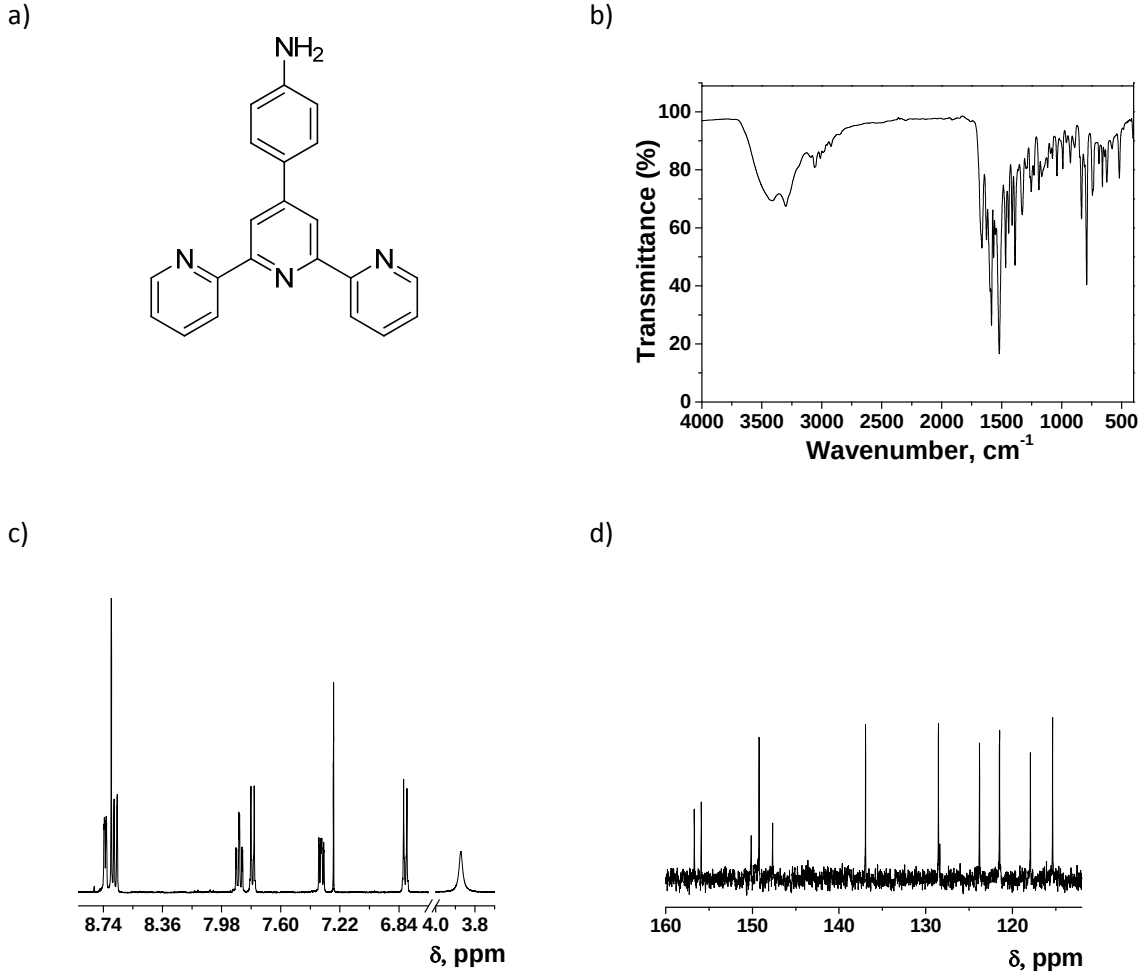

Figure S4. Characterisation of 4-(2,6-di(pyridin-2-yl)pyridin-4-yl)benzenamine (**4**): a) chemical structure; b) FT-IR; c) ^{1}H NMR; d) ^{13}C NMR (NMR solvent: DMSO-d_6).

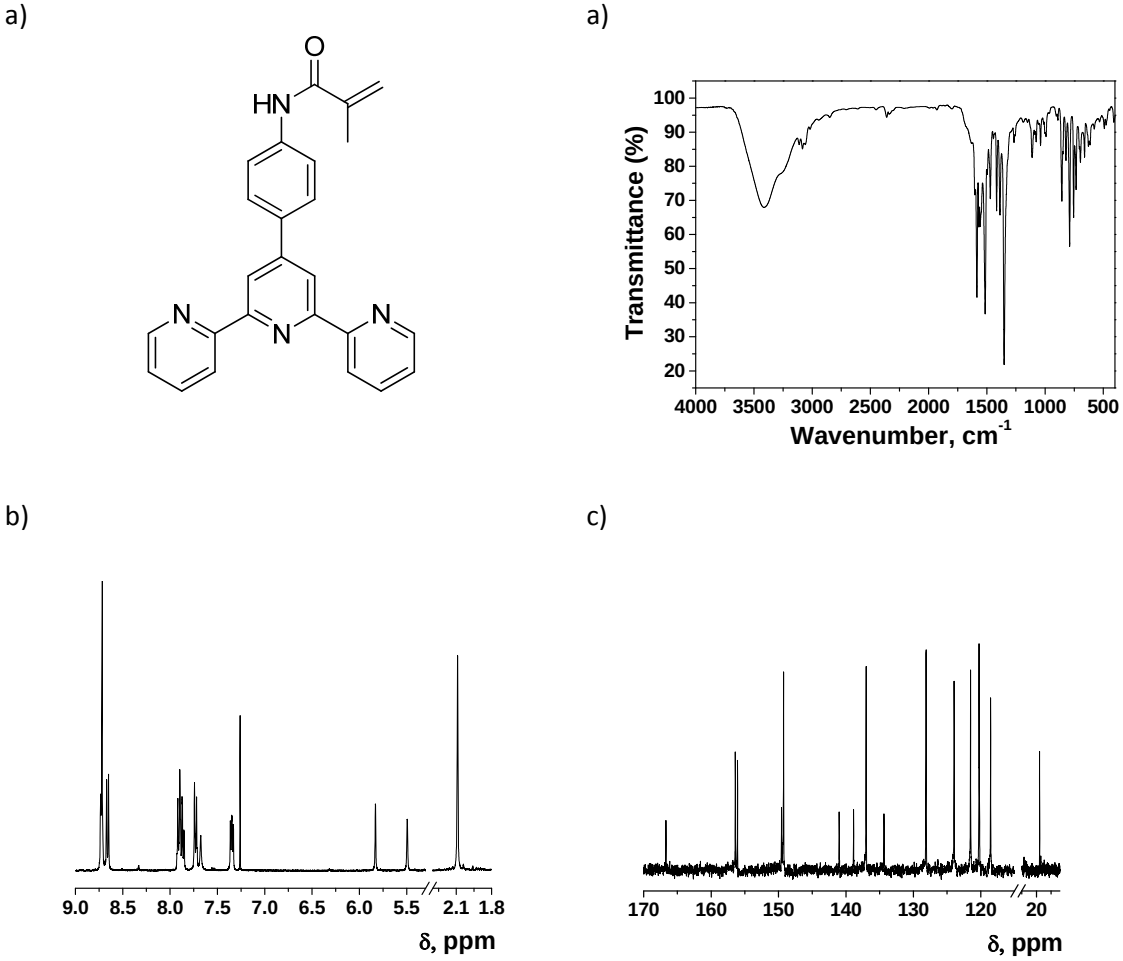

Figure S5. Characterisation of N-(4-(2,4-di(pyridin-2-y)pyridine-4-yl)phenyl)methacrylamide (**5**): a) chemical structure; b) FT-IR; c) ^{1}H NMR; d) ^{13}C NMR (NMR solvent: DMSO-d_6).

S2. Titration of Fe(III) with LCp

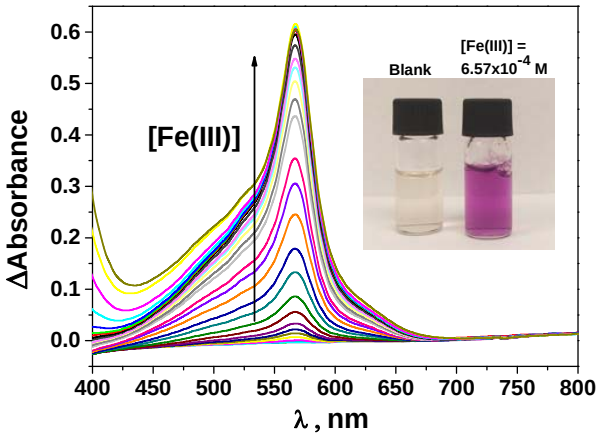

Figure S6. UV/Vis titration spectra of Fe (III) with a water solution of **LCp** (pH = 2, buffer = KCl-HCl, concentration of cations ranging from $6.75x10^{-8}$ to $6.57x10^{-4}$ M). The concentration of sensory motifs in water was $1x10^{-4}$ M (equivalents of pendant sensory tpy motifs per litre).

S3. Titration of Co(II) with LCp

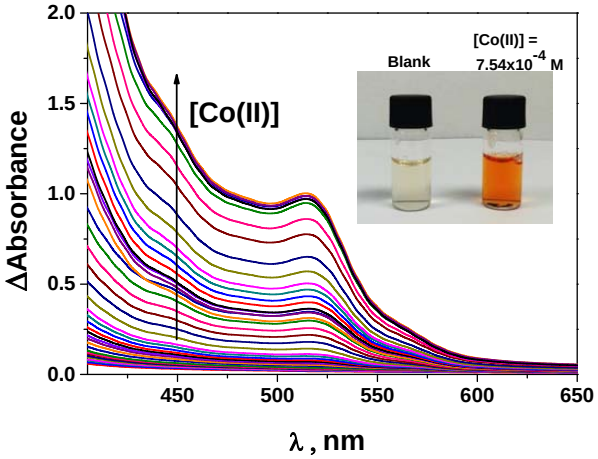

Figure S7. UV/Vis titration spectra of Co (II) with a water solution of **LCp** (pH = 2, buffer = KCl-HCl, concentration of cations ranging from $7x99{\cdot}10^{-8}$ to $7x54{\cdot}10^{-4}$ M). The concentration of sensory motifs in water was $1x10^{-3}$ M (equivalents of pendant sensory tpy motifs per litre).

S4. Titration of Cu(II) with LCp

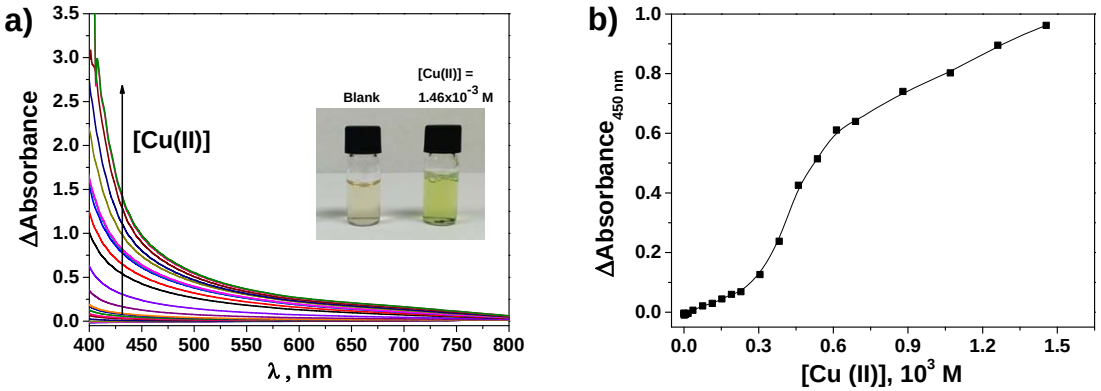

Figure S8. UV/Vis titration spectra (a) and curve (b) of Cu(II) with a water solution of **LCp** (pH = 2, buffer = KCl-HCl, concentration of cations ranging from $1.64x10^{-5}$ to $1.46x10^{-3}$ M). The concentration of sensory motifs in water was $1x10^{-3}$ M (equivalents of pendant sensory tpy motifs per litre).

S5. Titration of Sn(II) with LCp

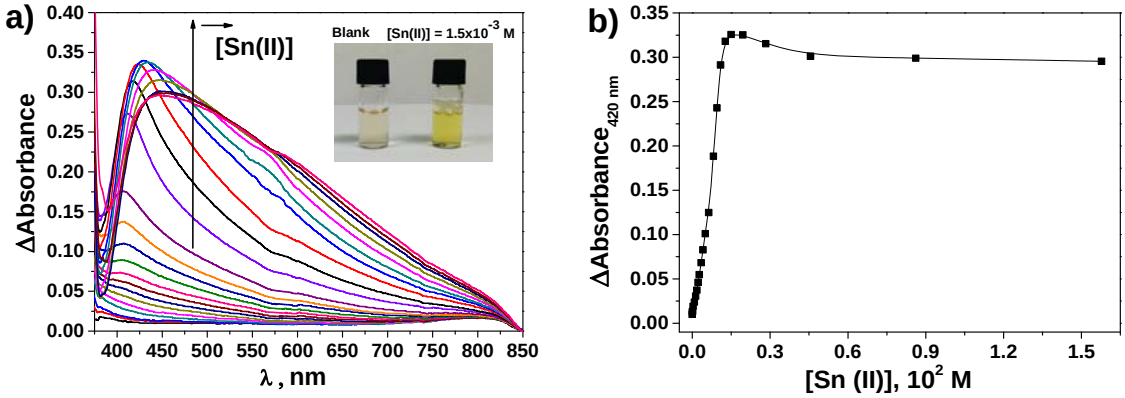

Figure S9. UV/Vis titration spectra (a) and curve (b) of Sn (II) with a water solution of **LCp** (pH = 2, buffer = KCl-HCl, concentration of cations ranging from $3.44x10^{-5}$ to $1.50x10^{-3}$ M). The concentration of sensory motifs in water was $1x10^{-3}$ M (equivalents of pendant sensory tpy motifs per litre).

S6. Titration of cations with pictures taken to Mem1 and Mem2.

The titration of Fe(III) and Co(II) with **Mem1** and Cu(II) and Sn(II) with **Mem2** was carried out with the colour data of pictures taken to sensory squares cut from the sensory membranes after immersing them in solutions of different concentrations of the cations in water. The quantitative studies were done using the digital photograph taken to sensory squares with a smartphone by treatment of the data of the color definition of each square (RGB parameters, R = red, G = green, B = blue). These parameters were obtained for each square directly after taking the photograph of the set squares through analysis with a conventional Android smartphone (app ColourMeter, automatically average 11 × 11 (121) pixels for each square). The three RGB parameters were reduced to one variable (principal component 1, PC1), using principal component analysis (PCA).

S6.1. Titration of Fe(III) with a picture taken to Mem1.

Table S1. RGB parameters and principal components obtained from the digital image of squares cut from the sensory membrane **Mem1** after immersion in water with Fe(III).

[Fe (III)], M	R	G	B	PC
$5x10^{-3}$	50	33	41	-1.95516
$1x10^{-3}$	41	29	43	-2.06522
$5x10^{-4}$	43	30	48	-1.98203
$1x10^{-4}$	80	42	83	-1.11377
$5x10^{-5}$	96	51	108	-0.597742
$1x10^{-5}$	140	108	147	0.811318
$5x10^{-6}$	154	131	156	1.26956
$1x10^{-6}$	169	160	165	1.79495
$5x10^{-7}$	170	161	164	1.8042
$1x10^{-7}$	177	172	169	2.03389

Table S2. Principal component analysis.

Component	Eigenvalue	Variance, %	Cumulative, %
PC1	2.94419	98.140	98.140
PC2	0.05381	1.794	99.933
PC3	0.0020027	0.067	100.000

Table S3. Component weights

Variable	PC1
R	0.582036
G	0.573253
B	0.576728

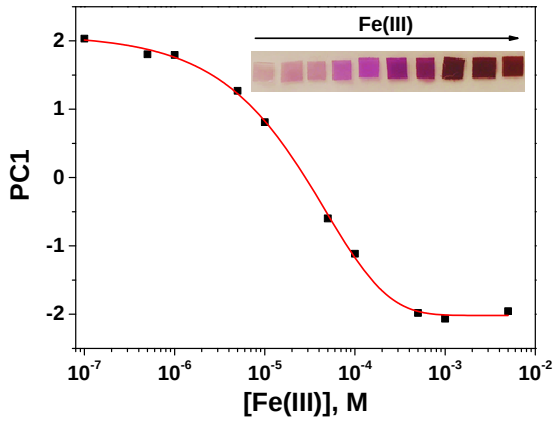

Figure S10. Titration curve of Fe(III) with **Mem1**. The digital color parameters (R,G and B) of each membrane square are group in one variable (principal component 1, PC1) by principal component analysis (PCA). Squares cut brom **Mem1** were immersed in water with concentration of Fe(III) ranging from $1x10^{-7}$ to $5x10^{-3}$ (pH = 2, buffer: KCl-HCl).

S6.2. Titration of Co(II) with a picture taken to Mem1.

Table S4. RGB parameters and principal components obtained from the digital image of squares cut from the sensory membrane **Mem1** after immersion in water with Co(III).

[Co(II)], M	R	G	B	PC
$5x10^{-3}$	156	89	44	-2.56815
$1x10^{-3}$	163	91	43	-2.15985
$5x10^{-4}$	170	94	45	-1.69921
$1x10^{-4}$	180	120	66	-0.458357
$5x10^{-5}$	184	144	95	0.511812
$1x10^{-5}$	183	163	131	1.20368
$5x10^{-6}$	182	165	138	1.26498
$1x10^{-6}$	180	173	155	1.4909
$5x10^{-7}$	176	173	158	1.30562
$1x10^{-7}$	172	173	160	1.10856

Table S5. Principal component analysis.

Component	Eigenvalue	Variance, %	Cumulative, %
PC1	2.53612	84.537	84.537
PC2	0.46185	15.395	99.932
PC3	0.00203299	0.068	100.000

Table S6. Component weights

Variable	PC1
R	0.514257
G	0.61889
B	0.59373

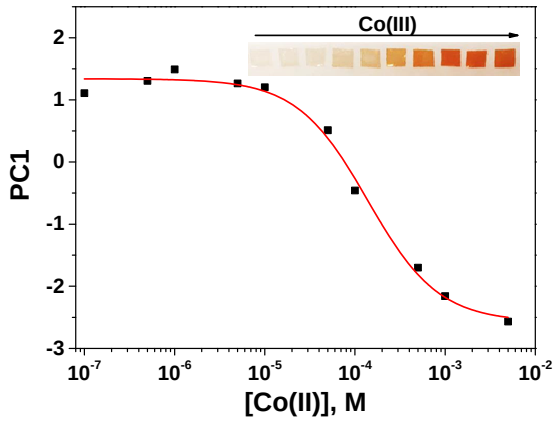

Figure S11. Titration curve of Co(II) with **Mem1**. The digital color parameters (R,G and B) of each membrane square are group in one variable (principal component 1, PC1) by principal component analysis (PCA). Squares cut brom **Mem1** were immersed in water with conentration of Co(II) ranging from $1x10^{-7}$ to $5x10^{-3}$ (pH = 2, buffer: KCl-HCl).

S6.3. Titration of Cu(II) with a picture taken to Mem2.

Table S7. RGB parameters and principal components obtained from the digital image of squares cut from the sensory membrane **Mem1** after immersion in water with Fe(III).

[Cu(II)], M	R	G	B	PC
$9x10^{-3}$	129	161	98	-2.64827
$6x10^{-3}$	140	170	108	-1.30406
$3x10^{-3}$	143	173	106	-1.07998
$9x10^{-4}$	161	179	121	0.456468
$6x10^{-4}$	169	182	126	1.09896
$3x10^{-4}$	174	182	131	1.44092
$9x10^{-5}$	180	183	140	2.03597

Table S8. Principal component analysis.

Component	Eigenvalue	Variance, %	Cumulative, %
PC1	2.91962	97.321	97.321
PC2	0.0757245	2.524	99.845
PC3	0.00465104	0.155	100.000

Table S9. Component weights

Variable	PC1
R	0.583573
G	0.571252
B	0.577161

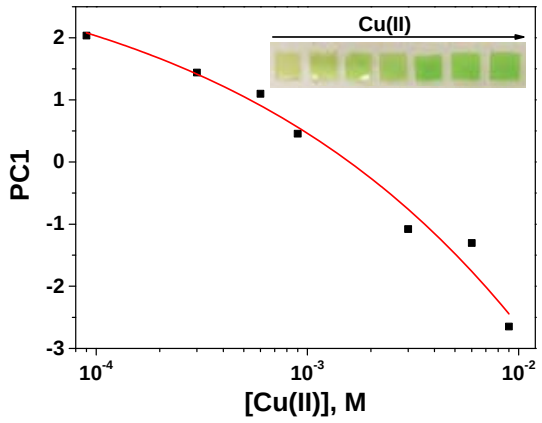

Figure S12. Titration curve of Cu(II) with **Mem2**. The digital color parameters (R,G and B) of each membrane square are group in one variable (principal component 1, PC1) by principal component analysis (PCA). Squares cut brom **Mem2** were immersed in water with conentration of Cu(II) ranging from $9x10^{-5}$ to $3x10^{-2}$ (pH = 2, buffer: KCl-HCl).

S6.4. Titration of Sn(II) with a picture taken to Mem2.

Table S10. RGB parameters and principal components obtained from the digital image of squares cut from the sensory membrane **Mem1** after immersion in water with Fe(III).

[Cu(II)], M	R	G	B	PC
$9x10^{-3}$	174	148	55	-2.40455
$6x10^{-3}$	179	154	64	-1.47304
$3x10^{-3}$	184	160	69	-0.619572
$9x10^{-4}$	187	169	82	0.365715
$6x10^{-4}$	191	176	95	1.33738
$3x10^{-4}$	186	179	111	1.35712
$9x10^{-5}$	181	179	138	1.43695

Table S11. Principal component analysis.

Component	Eigenvalue	Variance, %	Cumulative, %
PC1	2.36076	78.692	78.692
PC2	0.632503	21.083	99.775
PC3	0.00674105	0.225	100.000

Table S12. Component weights

Variable	PC1
R	0.504118
G	0.647955
B	0.570981

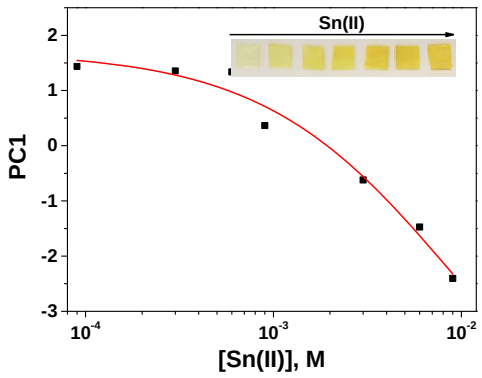

Figure S13. Titration curve of Sn(II) with **Mem2**. The digital color parameters (R,G and B) of each membrane square are group in one variable (principal component 1, PC1) by principal component analysis (PCA). Squares cut brom **Mem2** were immersed in water with conentration of Sn(II) ranging from $9x10^{-5}$ to $3x10^{-2}$ (pH = 2, buffer: KCl-HCl).

S7. Response time

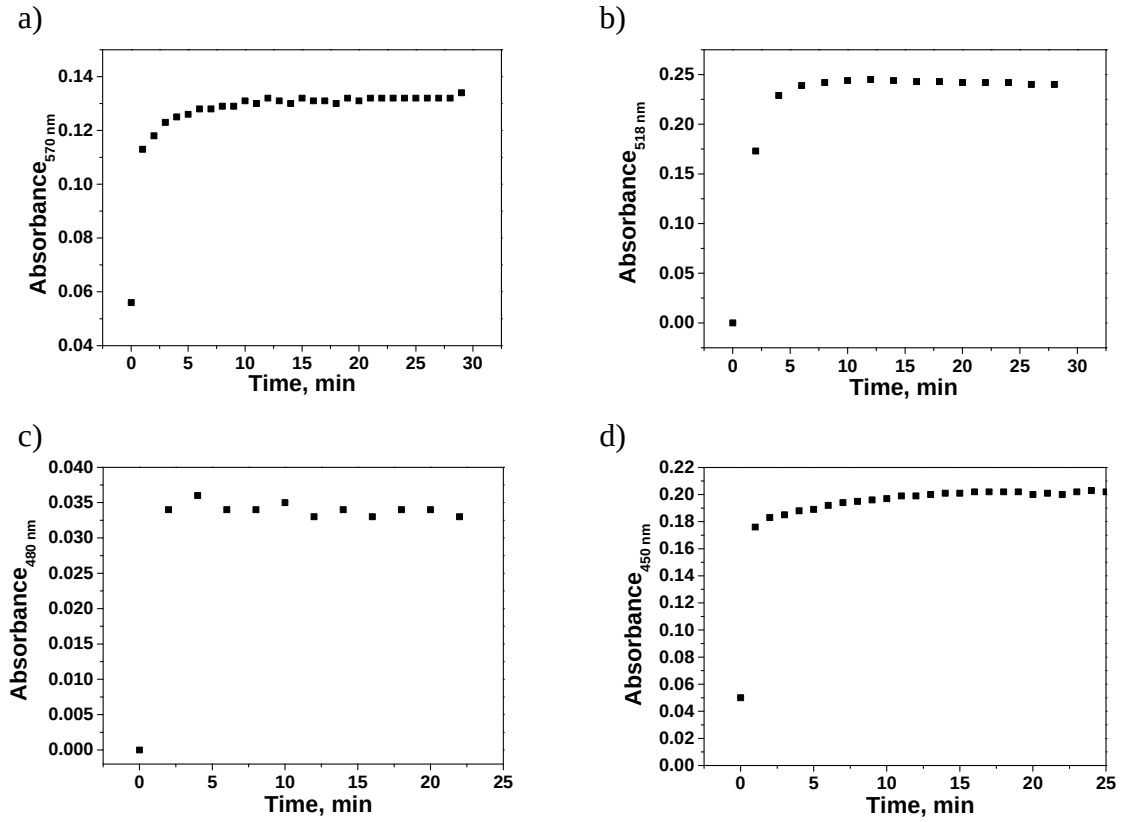

Figure S14. Response time. Absorbance of a solution of **LCp** in water (pH = 2, buffer: KCl-HCl) upon adding: a) Fe(III); b) Co(II); c) Cu(II); and d) Sn(II). The concentration of sensory motifs in water was $1x10^{-4}$ M for Fe(III), and $1x10^{-3}$ M for Co(II), Cu(II) and Sn(II) (equivalents of pendant sensory tpy motifs per litre). The concentration of each cation was $5x10^{-6}$, $5x10^{-5}$, $1x10^{-4}$ and $7.5x10^{-4}$ M for Fe(III), Co(II), Cu(II) and Sn(II) respectively.

S8. Interference study

a) b)

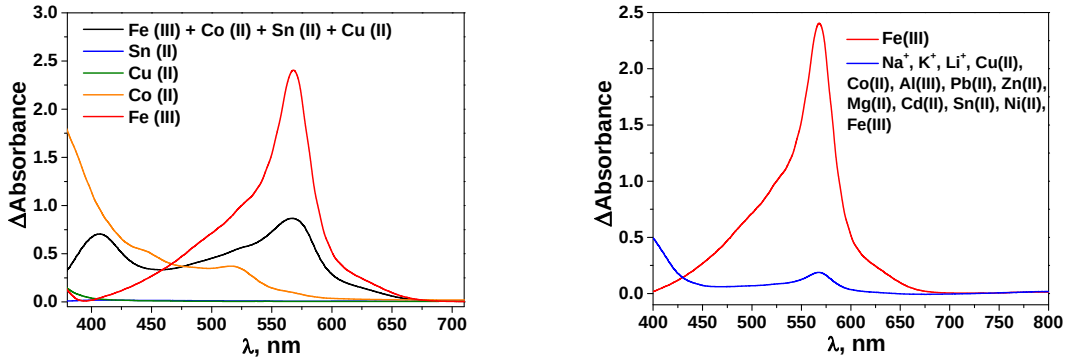

Figure S15. Interference study. Water solutions of **LCp** (concentration of sensory motifs was $1x10^{-3}$ M (equivalents of pendant sensory tpy motifs per litre)) upon adding a: a) cocktail of cations that forms coloured complexes with tpy motifs (Fe(III), Co(II), Cu(II), Sn(II). Concentration of each cation = $1.3x10^{-3}$ M); b) cocktail of 13 cations (Na^+, K^+, Li^+, Cu(II), Co(II), Al(III), Pb(II), Zn(II), Mg(II), Cd(II), Sn(II) and Ni(II), Fe(III), Cu(II), Co(II)). Concentration of each cation = $9.09x10^{-4}$ M).

a) b)

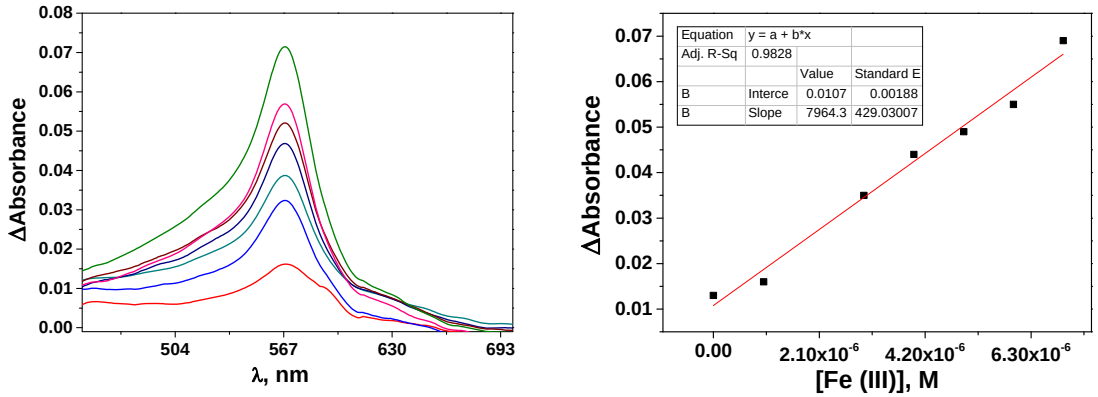

Figure S16. Standard addition of an aqueous solution of Fe (III) to a water solution of **LCp** (concentration of sensory motifs was $2x10^{-3}$ M (equivalents of pendant sensory tpy motifs per litre)) containing a cocktail of 13 cations (Na^+, K^+, Li^+, Cu(II), Co(II), Al(III), Pb(II), Zn(II), Mg(II), Cd(II), Sn(II) and Ni(II), Fe(III), Cu(II), Co (II)). The concentration of each cation was $1x10^{-6}$ M; b) least square fitting of the absorbance at 567 nm *vs* molar concentration of Fe(III). (Calculated concentration of Fe(III) = $1.3x10^{-6}$. Real concentration of Fe(III) and each cation = $1x10^{-6}$ M).